Are You There Gas? It's Me, Planet

The Effects of Gas on Growth of Gas Giant Cores through Planetesimal Accretion

A Thesis Presented
by

Natania R. Wolansky

to
The Department of Astronomy

in partial fulfillment of the requirements
for the degree of Bachelor of Arts

Advised by: Dr. Ruth Murray-Clay

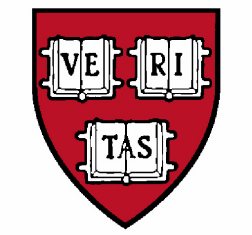

Harvard University
Cambridge, MA 02138
United States of America
April 11th, 2014

Abstract:

Before now, models have not been successful in predicting the rapid growth of rocky cores of gas giant planets at large separations from their host stars. Timescales for growth have far outstripped the lifetime of the gaseous disk surrounding the young star, creating a paradox between the need for the core to accrete material and the depleted supply of gas and dust. I present a model for planetary core accretion taking into account the effect of surrounding gas on the dynamics between the core and the accretable material, thus altering the characteristics of the effective cross section of accretion of the planet. By replacing the Hill radius with a wind shearing (WISH) radius, which tracks the point at which a small particle is not sheared away from a core by differential gas drag force, and by imposing additional energy constraints which determine whether a particle will successfully decouple from the gas during its encounter with the core, I recalculate the timescales of growth of a planetary core under a number of varying parameters. I apply the results to the A-type HR8799 star system, including HR8799b, c, and d, roughly 10M_J planets located at a separation of 68, 38, and 24 AU, respectively. Using the model, I reduce the "last doubling" timescales of growth predicted by classical gravitational focusing models by a factor of 1000, from 10^7 years to 10^4 years for HR8799b, c, and d, placing timescales of growth in all three cases within acceptable limits to agree with the lifetime of a gaseous disk and the deduced lifetimes of the planets. These results place within the realm of possibility that these 3 planets are formed by core accretion instead of gravitational instability. In exploring the timescales for growth of planetary cores in systems with varying parameters such as star size, disk density, and dust particle size distributions, I provide a model for predicting the possibility of driftless formation of a gas giant given the protoplanetary system's characteristics, which will help in future observational exoplanet discovery work.

Contents

Chapter 1

Introduction

1.1

One of the major focuses in astronomy has been to study our own solar system and the planets within it. We tackle problems such as the existence of gas giants like Jupiter and rocky planets like Earth, Mars, and Mercury to develop models that predict the huge diversity of astronomical objects in our immediate vicinity. Part of innate human curiosity is the desire to know where we came from, how our world came to be, and where it might be going. Studying planet formation is like studying the history of our world. Yet planet sizes and compositions vary, from tiny rocky planets to huge puffed-up balls of gas, planets on the verge of the ability to carry out nuclear fusion in their cores.

The recent development of projects like NASA's Kepler mission (Borucki et al., 2010) have spurred a newfound fascination with planetary studies by showing the variety of planetary systems, as well as exposing the fact that our own solar system may not be anything special. We have found that 70% of stars have planets with orbital periods at or less than Earth's (Fressin et al., 2013), a fact that holds promise for one day discovering life on other planets. In addition, Kepler has found many systems with familiar properties. In 2011, papers announced the discovery of the first rocky planet (Batalha et al., 2011), the discovery of a six-planet system (Lissauer et al., 2011) and the first roughly Earth-sized planets in 2012 (Fressin et al., 2012).

Similar to our own solar system, in most systems, the gas giants – if there are any – are located farther out than the rocky planets. According to Kepler's data, less than 3% of stars have

at least one gas giant within 1 AU (Batalha et al., 2013). Gas giants are perhaps some of the most interesting planets to study, as their huge size requires rapid accretion of gas early in the development of the solar system before available gas is blown away, likely by photo-evaporation (Alexander et al., 2006), on timescales of roughly a few million years (Jayawardhana et al., 2006).

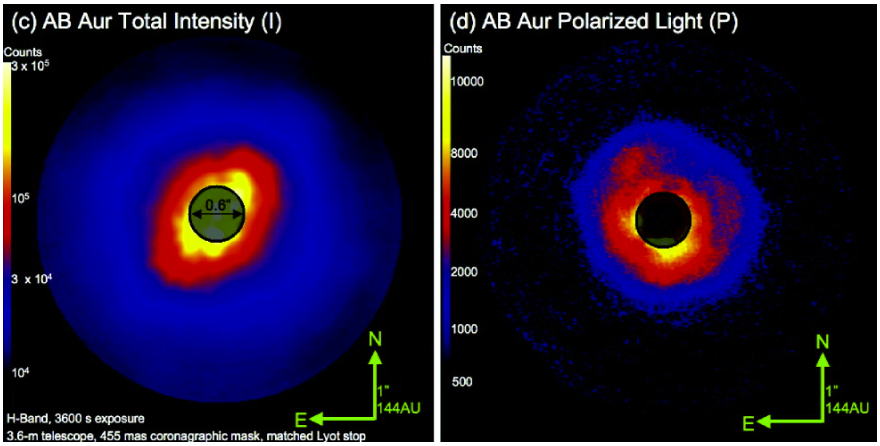

(a) An image of the circumstellar disk surrounding the young star AB Aurigae. Image taken using AEOS telescope on Haleakala, Hawaii. Image taken from Oppenheimer et al., 2008

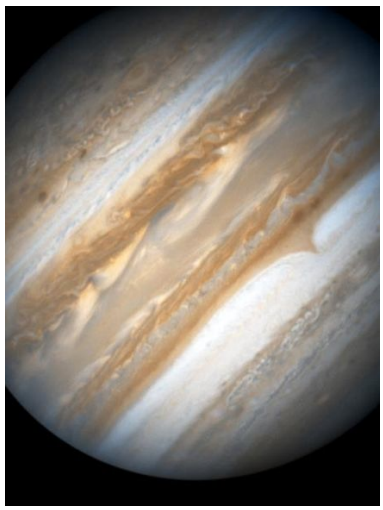

(b) An image of present-day Jupiter, courtesy of NASA/ESA/Hubble Heritage Team (AURA/STScI)

Dust and gas surrounding a young star provides the raw materials for the planets in that system. Image (a) above shows a typical intensity distribution of a circumstellar disk surrounding a young star. While material able to accrete onto a young core is abundant near the star, where the intensity of reflected light is high, the amount of material drops off as the distance from the central star increases.

With so many planets in our own solar system, one would think we know approximately how these planets came to form – the history of evolution from an a young solar disk like image (a) to image (b), modern day Jupiter. Yet despite this, the picture of how planets – both rocky and gaseous – come to be is far from complete.

1.2 Limits of Current Knowledge of Planet Formation

Four regimes exist for the formation of gas giants with varying methods of development for each regime:

1. Creation of small particles from the protoplanetary disk
2. Growth of small particles from roughly centimeter scales to kilometer scales
3. Growth of planetesimals from kilometer scales to scales about 10 times the mass of the Earth
4. Rapid acquisition of huge gaseous envelopes due to the gravitational influence of the core on the surrounding gas

The first regime, from a smooth disk to small particles, almost certainly comes about as the result of collisional coagulation due to Van der Waals forces (Ormel et al., 2007, see also Weidenschilling & Cuzzi, 1993). These particles then collide within the disk, sticking together upon collision to grow to about a centimeter in size (Dominik & Tielens, 1997. See also Blum & Wurm, 2000). Since the particles are almost all coupled to the surrounding gas (due to their small sizes) the relative velocities between them are small, mostly coming about simply due to Brownian motion. Thus, when they collide, the impact is low-energy and they tend to stick rather than fragment. In regime 2, the centimeter-sized particles settle to the mid-plane of the disk, allowing more collisions – and growth – to occur (Weidenschilling & Cuzzi, 1993). At about 1 meter in size, however, the objects couple less easily to the gas, creating relative velocities that, in a collision with another particle of similar size, will break the object rather than sticking to it. Furthermore, at this size, drag forces from the gas cause the particles to change direction, spiraling rapidly inwards towards the central star. This creates the "meter barrier" (Benz, 2000 and Weidenschilling, 1977). Growing particles from centimeter to kilometer size – thus moving past this barrier – is an open problem in planet formation.

This paper is primarily focused on the third regime, the growth of gas-giant cores from kilometer size to a size large enough to attract a gaseous envelope (about 10 m_{earth}). Two general models exist for this regime.

The first model uses gravitational instability as a catalyst. The 1-10 Jupiter-mass planet (depending on the temperature of the star and the separation from it) could have simply collapsed together, similar to the formation of stars from stellar nebula (Toomre, 1964). The problem with this model is that it tends to create objects larger than 10 Earth masses, mostly as binary brown dwarfs rather than gas giant planets (Kratter, Murray-Clay, & Youdin, 2011).

The other model assumes that a small core accretes grains of dust or smaller objects, catching them and building up mass as it travels in orbit around the central star. While this model could theoretically create a core of any size, it is limited by the amount of accrete-able material and the lifetime of the disk. Short lifetimes of the disk (Jayawardhana et al., 2006) and long core accretion times (Goldreich et al., 2004) put an upper limit on core sizes at large distances that doesn't agree with observational data. Standard core accretion models cannot even explain the growth of Uranus and Neptune, and even the most optimistic versions only allow for the formation of gas gians within 40-50 AU (Rafikov, 2004). This paper will attempt to solve the issues in this regime through a new version of core accretion, one that increases cross sections of accretion due to dynamical interactions with the surrounding gas in the disk.

1.3 Brief Overview of Core Accretion

In this section I will formulate a basic model of core accretion. Core accretion does not attempt to explain how protoplanets come to be (which is an open question in the astronomical community). Rather it describes how small cores grow to become larger by gravitationally colliding with and accreting small dust grains or planetesimals as it travels through the disk.

There are several conventional regimes in the core accretion model. A typical progression of stages in the model looks like:

1. Collapse of dust into cores
2. Runaway growth of large cores to roughly 100 km scales
3. Oligarchic growth
4. Rapid gas envelope accretion

In runaway growth, a larger core (moving at a low velocity due to energy equipartition) is surrounded in close proximity by smaller particles (moving at higher velocities) grows rapidly due to accretion (Wetherill & Stewart, 1989). In the oligarchic growth regime, cores are far enough away that gravitational forces influence velocities rather than self-stirring (Ida & Makino, 1993). Finally, once the core has reached about $10m_{earth}$ it enters the rapid gas envelope accretion phase where

gas, and not just dust, is accreted to form large, massive envelopes around the rocky core. The core spends most time in the oligarchic growth regime, where objects are accreted by gravitational (and gaseous) forces. This is the focus of my work.

In the oligarchic growth stage, a core will grow through accretion at a rate of:

$$\frac{\delta M_p}{\delta t} = \rho \pi {R_c}^2 v_c \tag{1.1}$$

Where M_p is the mass of the protoplanet, ρ is the density of accreteable material in the disk, R_c is the planet core's maximum radius of capture, and v_c is the velocity of an object (relative to the planet) located at the capture radius. Thus, the unknown parameter in determining the growth rate of the core is its capture radius.

In the absence of gas, particles are captured by gravitational focusing, where the gravity of the core pulls surrounding objects into collision courses. In this scenario, particles are accelerated during an encounter to velocity v_{Hill} associated with the Hill radius ($v_{Hill} = R_{Hill}\Omega$), the point at which the gravitational influence of the core on a particle overcomes the gravitational influence on that particle from the central star. Its mathematical definition is given by:

$$R_{Hill} = a \left(\frac{M_p}{3M_*} \right)^{\frac{1}{3}} \tag{1.2}$$

$$v_{Hill} = R_{Hill}\Omega \tag{1.3}$$

where a is the distance of the planetary core from the central star and Ω is its orbital frequency. One then finds the maximum radius, for a particle at this velocity, where the kinetic energy and angular momentum allow the particle to graze the core (creating a collision with the same angular momentum and energy as at infinity), and this radius, b, is the radius of accretion of the core. This idea will be developed further in coming sections.

1.4 Brief Overview of Gravitational Instability

Here I formulate a basic model of gravitational instability, the main competing theory to core accretion. Let a disk of gas have surface density Σ, angular velocity Ω, velocity dispersion c_s, and

pressure $P(\Sigma) \sim \rho {c_s}^2$ (with $\rho = \Sigma/H$ where H is the disk's scale height) (e.g. Chiang & Youdin, 2010). I define a value κ, the epicyclic frequency of radial oscillations, as:

$$\kappa = \sqrt{r\frac{\delta\Omega^2}{\delta r} + 4\Omega^2} \tag{1.4}$$

Using this definition, as well as the linearized equations for axisymmetric perturbations (e.g. Chiang & Youdin, 2010) the dispersion relation for asymmetric waves is given by:

$$\omega^2 = c_s^2 k_r^2 - 2\pi G\Sigma|k_r| + \kappa^2 \tag{1.5}$$

$$k_r = \frac{2\pi}{\lambda} \tag{1.6}$$

Here, the two positive terms of the dispersion relation serve to stabilize the disk and the negative term serves to destabilize the disk. In other words, when ω^2 is a negative number (and thus ω is imaginary), its behavior is exponential instead of sinusoidal. When wavelengths are short ($\lambda \ll 1$), k_r is large. In the limit of large k_r, the k_r^2 term dominates the $|k_r|$ term, so in order to keep ω^2 positive, one depends on the value of c_s (a function of pressure). When wavelengths are long ($\lambda \gg 1$), the relative values of $|k_r|$ and the k_r^2 term will determine whether ω is real or imaginary, so ω is dependent mainly on κ, a function of Ω. Thus, short wavelength oscillations are stabilized by pressure and long wavelength oscillations are stabilized by the rotation of the disk. For medium wavelengths, I define the Toomre criterion (Toomre, 1964) Q to be:

$$Q \equiv \frac{c_s\kappa}{\pi G\Sigma} \tag{1.7}$$

When $Q > 1$, medium wavelength oscillations are stabilized, but when $Q < 1$, medium wavelengths destabilize the gas, creating gravitational overpressures and underpressures that condense to gas giants (Boss, 2011).

1.5 Recent Observations – HR8799

Until recently, core accretion was generally accepted as the standard planet formation mechanism (e.g. Goldreich, Lithwick, and Sari, 2004). This was mostly because simple core accretion models

(such as those used in Fischer & Valenti, 2005) could account for planet formation and metallicity in planets within 5 AU of their star. At the time, this was no problem: most known exoplanets orbited within 3 AU of their star, well within the range of possibility in these models (Dodson-Robinson et al., 2009). It was known that these simple models were not perfect. Yet there was simply not enough data to be able to verify or falsify a new theory of core accretion or of any other method of planetary formation at large orbits.

HR8799

In 2008, however, direct imaging of star HR8799 showed three orbiting planets, at separations of 24 (planet d), 38 (planet c), and 68 AU (planet b) (Marois et al., 2008). The masses of the planets were determined and refined in a series of papers (Barman et al. 2011a, Currie et al., 2011, Galicher et al., 2011, Madhusudhan et al., 2011, and Marley et al., 2012) and summarized, as well as other planetary characteristics, in the table below, included in Marley et al., 2012:

Table 1
Summary of Derived Planet Properties

Planet	Ref.[a]	M ($M_{\rm Jup}$)	$\log g$	$T_{\rm eff}$ (K)	R ($R_{\rm J}$)	age (Myr)	$\log L_{\rm bol}/L_{\odot}$
b[b]	B11a	0.1–3.3	3.5 ± 0.5	1100 ± 100	0.63–0.92	30–300	-5.1 ± 0.1[c]
	C11	5–15	4–4.5	800–1000	...	30–300	
	G11	1.8	4	1100	0.69	...	
	M11	2–12	3.5–4.3	750–850	...	10–150	
	M12[d]	26	4.75	1000	1.11	360	-4.95 ± 0.06
c	C11	7–17.5	4–4.5	1000–1200	...	30–300	-4.7 ± 0.1[c]
	G11	1.1	3.5	1200	0.97	...	
	M11	7–13	4–4.3	950–1025	...	30–100	
	M12	8–11	4.1 ± 0.1	950 ± 60	1.32–1.39	40–100	-4.90 ± 0.10
d	C11	5–17.5	3.75–4.5	1000–1200	...	30–300	-4.7 ± 0.1[c]
	G11	6	4.0	1100	1.25	...	
	M11	3–11	3.5–4.2	850–1000	...	10–70	
	M12	8–11	4.1 ± 0.1	1000 ± 75	1.33–1.41	30–100	-4.80 ± 0.09

Figure 1.2: Table (taken from Marley et al., 2012, Figure 1) showing estimated characteristics of the three planets orbiting HR8799. One planet is predicted to be about 7 times the mass of Jupiter (Marois et al. 2010), the others about 10 times the mass of Jupiter. Temperatures for all three hover at about 1000 Kelvin.

Figure 1.2 shows that all three planets, each one farther than 20 AU, are many times the mass of Jupiter. This challenges core accretion models further, by constraining them to allow three giant planets to build up at large distances in a stable manner. Also, while core accretion models could not predict planets this large, the size and distance of the planets made models of gravitational instability that had previously been outside the realm of observed planets (e.g. Rafikov, 2005) now once again viable contenders for explaining the bizarre phenomenon. Put simply, the planets lie in a region between typical sizes and separations of the two models.

Furthermore, Marois' team, in 2010, announced the discovery of a fourth, closer-in planet orbiting HR8799, of comparable size to the other three (Marois et al., 2010). The planet, HR8799e, orbits at a radius of about 14.5 AU. The presence of four planets, all of large size, presents a challenge to the core accretion model, as well as rules out a scenario where the planets were formed closer to the star and later drifted away.

This raises several interesting points about planet formation. For example, the fact that HR8799 is an A-type star (as well as many other discovered stars with wide-separation gas-giant planets) opens discussion about the statistics of gas giants – star temperature correlation. Papers like Vigan et al. (2012) study the rates of massive, large-separation planets for several types of stars, from A-type to M-type, to determine whether the difference in frequency is a real phenomenon or simply observational bias.

HR8799 provides a perfect system as a testing ground for new models of core accretion. Since the planets lie in such an unexplored region, they provide an open source of data with which to test the boundaries of my new model. These planets and their properties will prove key to my understanding of the motivation of my research, as well as to checking the effectiveness of my new model.

1.6 Model using Gravitational Instability

Several papers have come out in favor of the gravitational instability hypothesis for the creation of planets such as those around HR8799. Dodson-Robinson et al. (2009) in particular arrive at this conclusion by attempting to rule out the two other possible mechanisms through numerical simulation as well as by simulating gravitational instability. Both planetary accretion and scattering

from the inner disk (where the planets are formed much farther in and then migrate outwards due to an interaction with a closer-in orbiting body) are ruled out based on the author's simulations.

The gravitational instability model presented is split into four necessary steps:

1. Disk breaks up into fragments
2. Each fragment is tracked through changes that occur over the lifetime of one orbit
3. The fragments accrete gas and dust
4. The fragments contract under their own self-gravity to spherical Jupiter-sized planets

and the paper outlines the physics behind the first step, allowing the disk to become gravitationally unstable enough for fragments to form.

The Dodson-Robinson paper makes use of models developed by Adams et al. (1989) and Laughlin & Rozyczka (1996) to find exponentially growing spiral modes, necessary for the gravitational instability. Finally, it produces the simulations shown below:

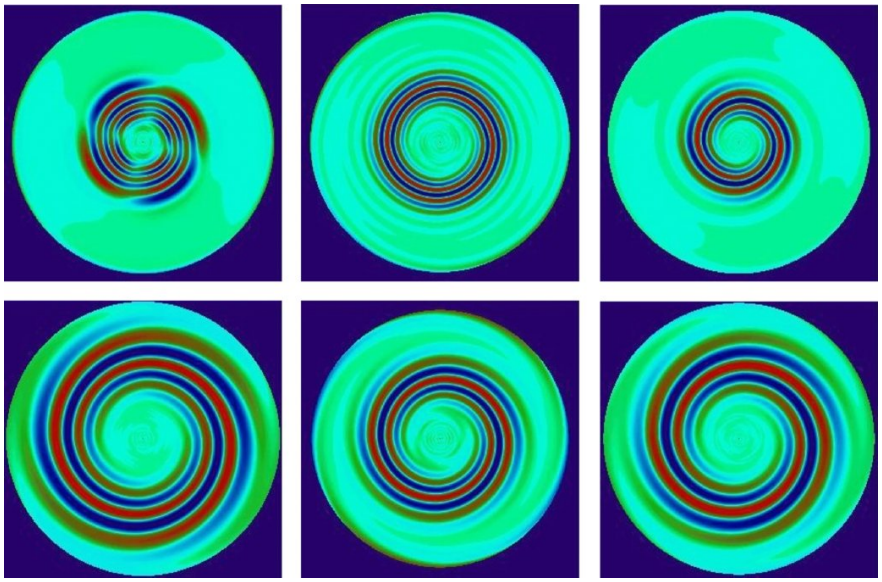

Figure 1.3: Taken from Dodson-Robinson et al., 2009 (Figure 3). The image shows the eigenmodes in the maximum-mass nebulae of three different type stars: A type (left), G type (middle), and M type (right). Red color corresponds to overdense regions, green in unaffected regions, and blue in underdense regions. In the case of the A type star, regions even far from the center are gravitationally unstable, and therefore capable of collapsing into a planetary core.

Dodson-Robinson shows a good attempt at the proof of the possibility of Gravitational Instability as the method for planetary formation. Kratter, Murray-Clay, and Youdin (2010), however,

state that in order for a planet-sized object to form from gravitational instability its host disk must be rapidly accreting. In such an environment, new fragments quickly grow too massive to be called planets. It is important to note that Dodson-Robinson never systematically proves the impossibility of core accretion. She simply assumes it (based on the gravitational focusing timescale issues).

1.7 Competing Models in Planetary Accretion

A few models have already been presented incorporating the presence of gas to try to solve the timescale problem in core accretion. In this section, I present two of the most important ones, noting the parts that will be useful for my own research, and parts where my research will differ. In doing so, I hope to give a sense of where the current research on the topic stands, and how my work will fit into the expanding body of knowledge on the subject.

Ormel & Klahr, 2010

Notably, Ormel & Klahr (2010) develop a model of growth of protoplanets involving gas drag. The model is correct in placing importance on the presence of gas in the process of protoplanet growth, especially when the core is less than about 10 Earth masses. The model makes several assumptions in order to make modeling and simulation easier. The assumptions are as follows:

1. The protoplanetary disk is flat enough to be modeled in 2D
2. Gas drag varies linearly with velocity
3. The disk is laminar, and has a smooth pressure gradient
4. Particles drift inwards radially
5. Protoplanets that are large in size are negligibly affected by gas drag, while small accreting particles do feel a force due to gas.

These assumptions allow easy simulation of the path of accreting particles, but also restrict the scope of the model. For example, by assuming gas drag varies linearly with velocity, the authors have limited themselves to modeling gas drag only in the Epstein and Stokes regime, and have neglected the RAM pressure regime, where gas drag varies quadratically with velocity. The authors

even state, "In fact, there is a transition regime between the Stokes and quadratic [RAM pressure] regimes where stopping times are proportional to $|\Delta v|^{0.4}$ which we have, for reasons of simplicity, ignored here" (Ormel & Klahr, 2010). In my model, no gas drag regime will be ignored or excluded.

Ormel and Klahr then go on to use full 3-body integrations, including added gas drag, to simulate some possible paths of objects surrounding a core. Below is shown Figure 5 from that paper, which demonstrates some of the paths approaching particles might take:

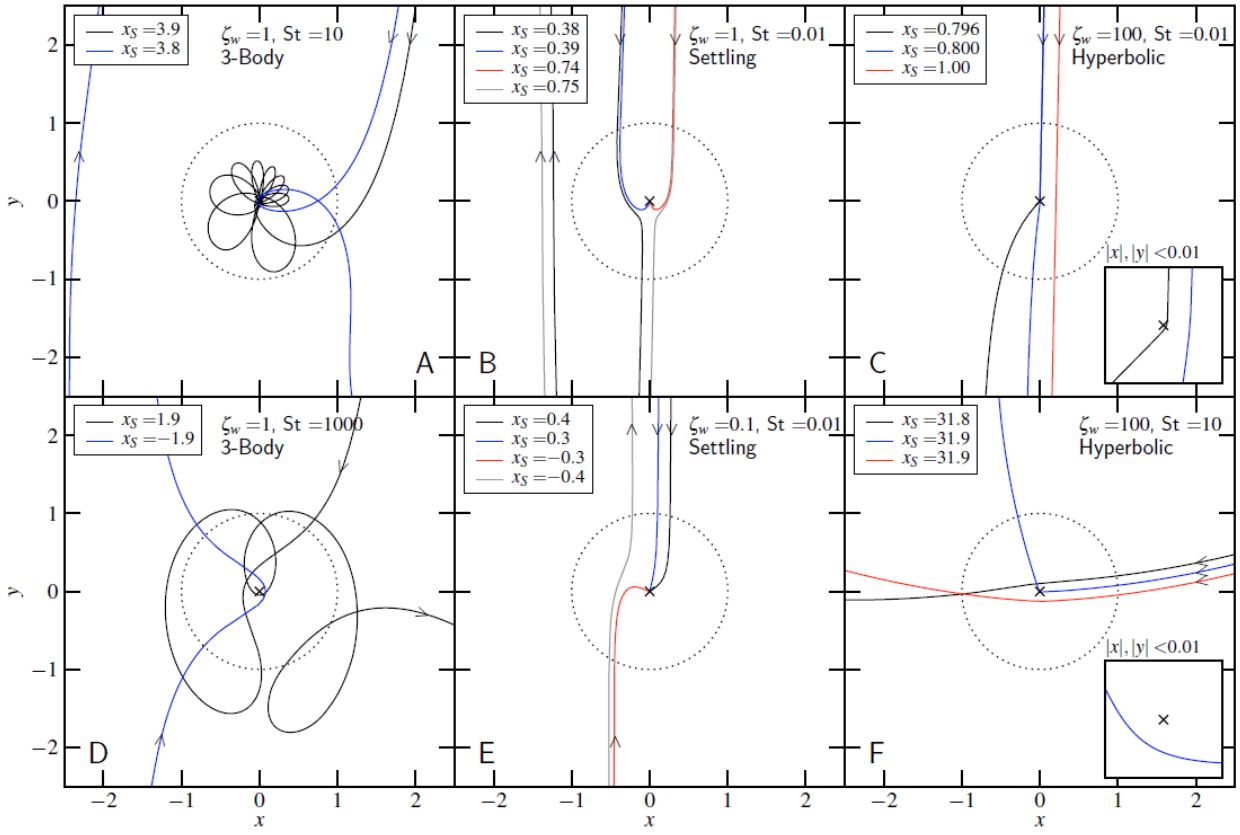

Figure 1.4: Taken from Ormel & Klahr, 2010 (Figure 5). Different scenarios of particle capture/ejection are presented, showing how small variations in starting position of the particle have large impacts on the possibility of capture of the particle. ζ_w represents the headwind velocity of the surrounding gas and St represents the "coupling parameter," a value defined in the paper. The dotted circle represents the Hill radius of the core.

Using the three scenarios shown in the figure (3-body, settling, and hyperbolic) the authors go on to classify impact parameters for each scenario, combining these to find growth timescales of the core.

My model differs from the Ormel & Klahr paper in a few ways. First, rather than try to model the exact path of a particle as it encounters the core, I simply model the parameter space to find

which parts of the parameter space lead to accretion and which lead to rejection. From there, I can model planet growth without needing to map out the trajectories of every single particle in the system.

More importantly, the dotted circles in Figure 1.5 point to the most fundamental difference between my work and the authors of this paper's work. While they talk about shearing due to gas, they still use the Hill radius as an indicator of the region of stability surrounding a planetary core. The Hill radius, however, is a notion firmly rooted in Kepler's gravitational laws and 3-body motion in a gas-free environment. I prove that for some parts of parameter space, objects within the Hill radius may still not be stable, due to shear caused by varying velocity with respect to the disk of gas. The authors get to this point, but in a roundabout and complicated way which, I believe, is the reason they had to make other limiting simplifications, such as with the linear gas drag regime. I will prove that by simply replacing the Hill radius with the WISH (Wind Shearing) radius where it is smaller than the Hill radius, one can model the stability of a particle entrenched in gas, no matter its velocity in relation to the gas.

Furthermore, the Ormel & Klahr paper only applies their model to a core at a distance of 5 AU. Because of my observational goal regarding the planets in HR8799, I apply my model out to much larger distances, where disks are less dense and therefore planetary accretion becomes more difficult. A major piece of my work is exploring the effect of gas drag on different planetary systems, attempting to find regions that, under particular conditions, are particularly efficient at accreting mass. Thus the scope of my work is much broader than in the Ormel & Klahr paper.

Lambrechts & Johansen, 2012

More recently, Lambrechts & Johansen (2012) present another model for protoplanetary accretion. This model is actually quite similar to the model I present. They use the presence of gas around centimeter-sized particles, which they call "pebbles" to model gas drag forces. Again, they make the assumption that the core is moving on a circular, Keplerian orbit around its star (the same assumption was made in Ormel & Klahr and in my research as well).

The paper models accretion by assuming that a pebble, entrained in gas, will only accrete if it is able to dissipate enough energy to be released from the gas flow (Lambrechts & Johansen, 2012). Thus, unlike Ormel & Klahr's modeling of a specific trajectory of a particle, it sets limits

to the energy a particle can have, at what distance from the growing core, in order to free itself of gas coupling and be pulled into collision. By varying the size of the growing core, Lambrechts and Johansen characterize two core regimes. The first, the so called "drift regime" in which the following relation holds:

$$M_c < M_t \tag{1.8}$$

$$M_t = \sqrt{\frac{1}{3}} \frac{\Delta v^3}{G\Omega_K} \tag{1.9}$$

Where M_t refers to the mass where the Bondi radius is similar in size to the Hill Radius. In this "drift regime," pebbles are essentially coupled to the gas, and thus approach the planetary core at the same velocity as the gaseous headwind. If the core mass is larger, however, the pebbles will not be so entrenched with the gas.

Finally, they present the results of their work in a graph, shown below:

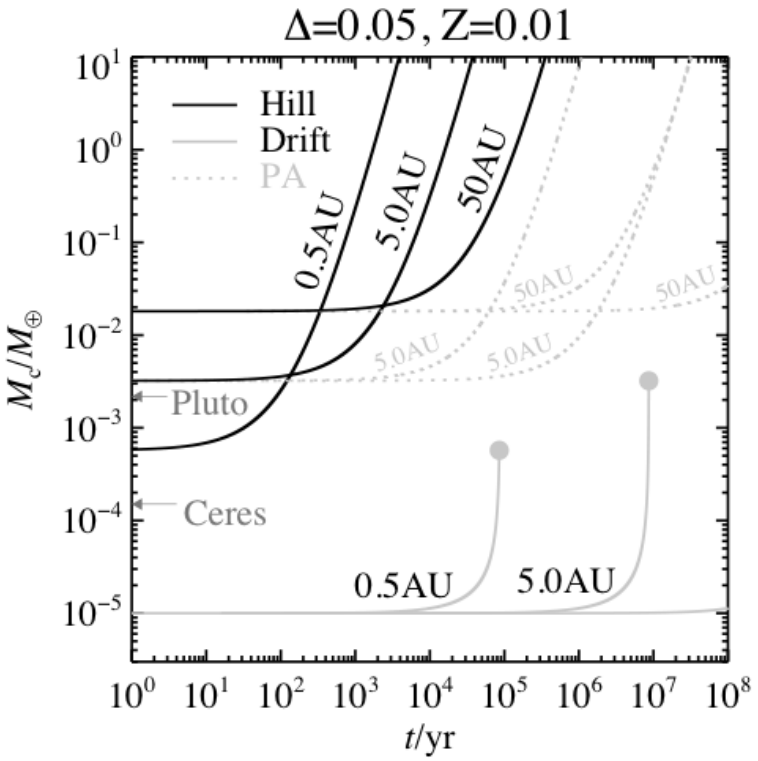

Figure 1.5: Results of Lambrechts & Johansen, 2012 (Figure 11 in the paper). Core growth (shown as a fraction of Earth's mass) as a function of time, for three different models. The drift branch represents growth in the drift regime, cut short and transferred to the Hill regime at $M_c = M_t$. PA represents classical, gas-free planetary accretion models.

While Lambrechts and Johansen (2012) will certainly prove useful as a comparison to my work, it differs in two significant ways. First, similarly to the Ormel and Klahr paper, the Lambrechts and Johansen paper uses the Hill Radius as a comparison, rather than the WISH radius. This proves to be a significant difference especially at smaller distances from the star, due to thicker gas. I only use the Hill Radius when it is smaller than the WISH radius.

Also, this paper limits itself in parameter space, first by assuming that all pebbles are 1 cm in radius, and by limiting the scope of parameter space it explores. The model is only tested at 0.5 AU, 5.0 AU, and 50 AU – leaving a large region left to be explored. My model, in addition to making use of the WISH Radius, attempts to explore protoplanetary environments in a more robust way, to provide a picture, and not just a small sample, of the possibilities of planet growth around a certain type of star.

1.8 Layout of the Paper

My research, as explained above, seeks to provide a flexible model of core accretion in a variety of protoplanetary disk environments. Allowing the model to accommodate many different stars, planetary cores, and gaseous environments makes it an important tool for predicting possible locations of large exoplanets in known stellar systems, as well as a good way to find orbital systems that are unusual – that is, where large planets exist in locations not especially conducive to large planet formation. My thesis is organized in the following order:

1. Background Derivations

   In this section, I provide the derivations for many of the important values in core accretion – for example, the Hill Radius, gas drag laws in different regimes, and Keplerian orbital dynamics, along with corrections due to gas pressure. This helps to give the reader an intuitive sense of how adding gas changes the dynamics of the system and helps to clarify the specific meaning of terms used. Because the model is essentially based around gas drag, a majority of the chapter focuses on developing a framework of how different sized objects are affected by the presence of gas.

2. Steps to Modeling

This section explains, step by step, the development of my model for determining the cross-section for core accretion, given certain environmental parameters. The model works by the following: a test particle, at a certain distance and velocity, is presented with a number of "tests" (such as being energetic enough to be able to decouple from the gas and being within the WISH radius of the core) which, if any are failed, would result in a failure to accrete onto the core.

By building up a capture radius through testing the accretability of a test particle at various separations from the core, an area of accretion is created, which differs based on core size and test particle size. This area of accretion, when plugged into the appropriate timescale formula, gives a net growth rate of the core, and thus a timescale of growth can be calculated for that core. By going through and describing each step in model development, I elucidate the process by which a particle accretes onto a core, and where (and why) things go awry.

3. Model Visualization in Parameter Space

   Next, I generalize the model, doing simulations that cover different star types, as well as different distances of cores. In doing this, I predict, for a certain type of star and disk density, where large planets are most likely to form from core accretion. This will be a powerful tool for observers, because it will narrow down for them where to look for large exoplanets (if knowledge about the system's early characteristics can be gleaned). I am able to find out whether certain bands around certain stars are best for planet growth, or, like has been suggested (Vigan et al., 2012) whether wide-orbit planets are much more common in general around a certain type of star, such as A-stars.

4. Case Study: HR8799

   Finally, I apply my results to planetary system HR8799, plugging in the stellar mass, disk properties, and distances of the three far away planets (Marley et al., 2012) to see whether my model predicts the possibility of formation of planets of this size at this distance. This is a good test of the model, because observations have already been made (Marois et al., 2008) of the three planets and their distances through direct methods. If the model predicts the possibility of planets at those distances, one could theoretically use the timescale of growth

(at that distance) to estimate the age of the planets. This is useful, as there has been much research lately into the age of the planets in the system (e.g. Sudol & Haghighipour, 2012) that can be further validated using my model. Using HR8799 is a good capstone to prove the efficacy and the applicability of the model developed in this paper.

Chapter 2

Background Physics

2.1 Derivation of the Hill Radius

One cannot study planetary accretion without mention of the Hill radius. Essentially, it describes the spot between two objects at which a test particle will switch "orbits" – will feel the same gravitational force from the smaller object as tidal gravitational force from the larger. In a system where particles did not feel a drag force from a surrounding gas environment, the Hill radius (and associated Hill velocity) would be a good approximation for the minimum velocity at which an incoming particle is moving as it is gravitationally focused into a collision – and in fact, the use of this Hill radius for just that purpose led to the timescale of growth paradox in the first place. I will now derive the equation for the Hill radius, for use later on in the model.

Let two objects be in orbit, separated by a distance a. The larger object (a star) has a mass M_* and the smaller (a planet) has a mass m and a radius r. The Hill radius is the distance at which the gravitational influence of the planet becomes comparable to the tidal perturbation by the star. Let that distance be given by d (measured from the planet). The force per mass (f) due to gravitational force on the planetesimal from the planet core can be given by:

$$f = \frac{Gm}{d^2} \tag{2.1}$$

Furthermore, the tidal perturbations by the star can be represented by:

$$\Delta f = \frac{GM_*}{(a-x)^2} - \frac{GM_*}{a^2} \tag{2.2}$$

Setting these two equal, I arrive at the expression:

$$\frac{Gm}{d^2} = \frac{GM_*}{(a-d)^2} - \frac{GM_*}{a^2} \tag{2.3}$$

I assume that $d \ll a$. Therefore, I can Taylor expand the right hand side of the equation (keeping only the first term), simplifying the equation to:

$$\frac{Gm}{d^2} = \frac{2M_*d}{a^3} \tag{2.4}$$

Solving for d, I arrive at an approximate expression for the Hill Radius (assuming $m \ll M_*$):

$$d = \left(\frac{m}{2M_*}\right)^{1/3} a \tag{2.5}$$

A more exact calculation yields:

$$d \approx \left(\frac{m}{3M_*}\right)^{1/3} a \tag{2.6}$$

The exact derivation requires using a reference frame rotating along with the planet at angular velocity Ω. However, the intuition used in this derivation is, for my purposes, correct and instructive for future uses of the Hill radius in this paper.

2.2 Radius of Accretion in Gas-Free Gravitational Focusing

In this section, I explain how to find the accretion radius in a gas-free environment through the mechanism of gravitational focusing. The following figure describes the parameters important to the problem:

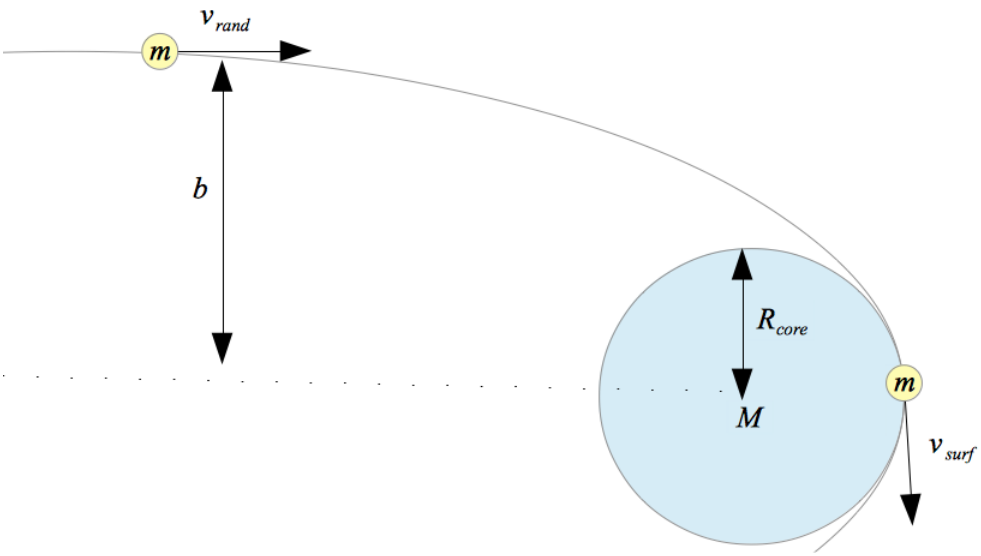

Figure 2.1: Diagram showing a setup to help determine the radius of accretion, b, in a gravitational focusing, gas-free model.

Imagine a (stationary) core with radius R_{core} and mass M. Imagine a particle approaching the core at a height of b, with mass m, moving at velocity v_{rand}. In order to find the distance, b, which supports focusing to collide with the core, I simply equate the angular momenta and the energies of the particle in the two locations. Assume 0 potential energy at ∞.

Far away, the particle has energy (E) and angular momentum (L):

$$E = \frac{1}{2}mv_{rand}^2 \tag{2.7}$$

$$L = bmv_{rand} \tag{2.8}$$

At the surface of the core, the particle has energy and angular momentum:

$$E = \frac{1}{2}v_{surf}^2 - \frac{GM}{R_{core}} \tag{2.9}$$

$$L = R_{core}mv_{surf} \tag{2.10}$$

Equating the two angular momenta yields:

$$bv_{rand} = v_{surf}R_{core} \tag{2.11}$$

$$v_{surf} = \frac{bv_{rand}}{R_{core}} \tag{2.12}$$

Furthermore, equating the two energies yields:

$$\frac{1}{2}v_{rand}^2 = \frac{1}{2}v_{surf}^2 - \frac{GM}{R_{core}} \tag{2.13}$$

Plugging in for v_{surf} gives:

$$\frac{1}{2}v_{rand}^2 = \frac{1}{2}\frac{b^2v_{rand}^2}{R_{core}^2} - \frac{GM}{R_{core}} \tag{2.14}$$

Using the definition for escape velocity I manipulate this equation algebraically into something elegantly simple:

$$v_{esc} = \sqrt{\frac{2GM}{R_{core}}} \tag{2.15}$$

$$\frac{GM}{R_{core}} = \frac{1}{2}v_{esc}^2 \tag{2.16}$$

$$v_{rand}^2 = \frac{b^2v_{rand}^2}{R_{core}^2} - v_{esc}^2 \tag{2.17}$$

$$\frac{b^2}{R_{core}^2} = \frac{v_{rand}^2 + v_{esc}^2}{v_{rand}^2} \tag{2.18}$$

Finally, I arrive at the equation:

$$\frac{b^2}{R_{core}^2} = 1 + \left(\frac{v_{esc}}{v_{rand}}\right)^2 \tag{2.19}$$

For the gravitational focusing model, an encountering particle is entering the Hill radius of the core. If the incoming velocity of the particle is larger than the escape velocity of the core, that is to say $v_\infty \geq v_{esc}$ then the radius of accretion is approximately R_{core} ($b \approx R_{core}$) and the planetary core only accretes that which directly collides with it. If $v_\infty \leq v_{Hill}$ then the particle will be accelerated to v_{Hill} (see Chapter 2.8 for an explanation of this) so v_{rand} will be v_{Hill}. Between those two values,

the incoming velocity of the particle will be unaffected during its encounter so $v_{rand} = v_\infty$. Here I assume that v_{Hill} is given by:

$$v_{Hill} = \sqrt{\frac{GM}{R_{Hill}}} \tag{2.20}$$

In my calculations, I use the standard choice of setting $v_\infty = v_{Hill}$, assuming there is a high probability of a particle having been excited to that velocity during a previous encounter with the core. Thus, I assume that:

$$v_{rand} = \sqrt{\frac{GM}{R_{Hill}}} \tag{2.21}$$

Now the equation for the accretion radius in the gravitational focusing model is complete. Because the radius of accretion is b, the area of accretion is πb^2.

2.3 Derivation of Scale Height

I now will derive a formula for the scale height of a disk (essentially the thickness of gas), another important quantity that will be used to develop some of the fundamentals of my model.

For a given particle, let a represent the radial distance from the star, and let z represent the distance from the plane. Using cylindrical coordinates, the gravitational force exerted on that particle from the star can be represented by:

$$F_g = \frac{GmM_*}{a^2}\left(-sin\left(\alpha\right)\hat{z} - cos\left(\alpha\right)\hat{r}\right) \tag{2.22}$$

where α is the angle between the plane and the particle, from the perspective of the star. Now, assuming that $z \ll a$ I can replace

$$sin(\alpha) \approx \frac{z}{a} \tag{2.23}$$

$$cos(\alpha) \approx 1 \tag{2.24}$$

Thus, the equation now becomes

$$F_g = \frac{GmM_*}{a^2}\left(-\frac{z}{a}\hat{z} - \hat{r}\right) \tag{2.25}$$

The radial component of this force is cancelled out by the centrifugal force on the particle due to the rotation of the disk. The vertical component of the force I must balance, using the assumptions that the disk is supported by pressure and that it is in hydrostatic equilibrium.

Using the force due to gravity in the $\hat{z}$ direction and the fact that the gas is in hydrostatic equilibrium, the change in pressure per z is given by:

$$\frac{\delta P}{\delta z} = -\frac{GM_*\rho(a)z}{a^3} \tag{2.26}$$

(Consider a box of height δz. The difference between the force on the top and the force on the bottom is scaled by a factor of δz, since pressure is defined as the force per area).

The pressure P, assuming an isothermal gas, is given by $P = c_s^2\rho(a)$ where $\rho(a)$ represents the density of the gas at a. Plugging in for pressure,

$$\frac{\delta\rho(a)}{\delta z} = -\frac{GM_*\rho(a)z}{c_s^2 a^3} \tag{2.27}$$

Solving this differential equation, I get:

$$\rho_a(z) = \rho(0)e^{-\frac{GM_*z^2}{2c_s^2a^2}} = \rho(0)e^{-z^2/2H^2} \tag{2.28}$$

where H, the scale height, is $\left(\frac{a^3c_s^2}{GM_*}\right)^{1/2}$. In order to find Ω, I invoke Kepler's third law, which states that the square of the orbital period is proportional to the cube of the orbital radius. Using this relation, I arrive at the relation:

$$G(M_* + M_p) = \Omega^2 a^3 \tag{2.29}$$

Assuming $M_* \gg M_p$, I can simplify this to:

$$GM_* = \Omega^2 a^3 \tag{2.30}$$

$$\Omega = \left(\frac{GM_*}{a^3}\right)^{1/2} \tag{2.31}$$

Substituting in Ω, the result is:

$$H = \frac{c_s}{\Omega} \tag{2.32}$$

2.4 Orbital Velocity Change Due to Presence of Gas

Now I will dive into some of the specific physics of the model. Mostly, I use a Keplerian framework when describing the dynamics of the star-planetary core system. I must make a few corrections, however, to account for the presence of gas, and the effect this will have on the motions of the relevant objects. First, I look at the rotation of the gas itself.

Normally, when describing the circular orbit of a gas particle around a star, one would simply use the Keplerian orbit – that is to say, following Kepler's laws. The gravitational force acting on that gas particle from the star is given by:

$$F_g = \frac{GM_*m}{r^2} \tag{2.33}$$

where m represents the mass of the particle, and r represents the distance to the star from the object. I then set this equal to the centripetal acceleration, yielding the equality:

$$\frac{v_{kep}^2 m}{r} = \frac{GM_*m}{r^2} \tag{2.34}$$

$$\frac{v_{kep}^2}{r} = \frac{GM_*}{r^2} \tag{2.35}$$

thus getting a relation for Keplerian velocity independent of the mass of the particle. However, with a gas particle in a gaseous disk, the gravitational force is not the only force acting on the particle. Because the gas feels the pressure of the disk pushing outwards, its velocity will therefore

be less than the Keplerian velocity:

$$v_{gas} < v_{kep} \tag{2.36}$$

One can think of this force as caused by the difference in force on either side of the "box of gas." This difference in force causes an acceleration towards the side of lower pressure (outwards). Consider a cube of gas with density ρ, length δr, and surface area δA. The force acting on each side of the cube is the pressure multiplied by the surface area, or $P(\delta A)$.Thus, the difference in force acting on one side of the cube and the other can be described by:

$$\Delta F = (\Delta P)(\delta A) \approx (\delta P)(\delta A)$$

The mass of the cube of gas is given by:

$$m_{cube} = \rho(\delta A)(\delta r)$$

Then using $F = ma$ I plug in:

$$a_{gas} = \frac{\Delta F}{m_{cube}} \tag{2.37}$$

$$a_{gas} = \frac{1}{\rho}\frac{\delta P}{\delta r} \tag{2.38}$$

$$a_{centripetal} = a_{gravity} + a_{gas} \tag{2.39}$$

$$\frac{v_{orb}^2}{r} = \frac{GM_*}{r^2} + \frac{1}{\rho}\frac{\delta P}{\delta r} \tag{2.40}$$

where a_{gas} represents the acceleration of the gas due to these forces. Let's convert this result into a more familiar form, using some assumptions about the behavior of the body. First, I solve the equation for v_{gas}, yielding:

$$v_{gas} = \sqrt{\frac{GM_*}{r} + \frac{r}{\rho}\frac{\delta P}{\delta r}} \tag{2.41}$$

In a gaseous disk, the pressure can be described by:

$$P = cr^n$$

where c and n are constants and in the case of a large disk, n is very close to -1. Thus, differentiating:

$$\frac{\delta P}{\delta r} = c(n-1)r^{n-1} \tag{2.42}$$

$$\approx \frac{-nP}{r} \tag{2.43}$$

$$\approx \frac{-P}{r} \tag{2.44}$$

Thus, the correction to the orbital velocity, Equation 2.38, can be approximated by:

$$a_{gas} = \frac{P}{\rho} \tag{2.45}$$

I assume the gas is approximately ideal and use the equations:

$$PV = nKT \tag{2.46}$$

$$c_s = \sqrt{\frac{KT}{\mu}} \tag{2.47}$$

where c_s is the speed of sound in that gas, K is the Boltzmann constant, T is the temperature of the gas, n is the number of particles, and μ is the molecular mass, or mass per particle. Combining equations 2.46 and 2.47:

$$\frac{P}{\rho} = \frac{VP}{m} = \frac{nKT}{m} = \frac{KT}{\mu} = c_s^2 \tag{2.48}$$

The Keplerian velocity is defined to be:

$$v_{kep} = \sqrt{\frac{GM_*}{r}} \tag{2.49}$$

Combining this with equations 2.41 and 2.48, I now rewrite the orbital velocity as:

$$v_{gas} = \sqrt{v_{kep}^2 - c_s^2} \tag{2.50}$$

Or, in an equivalent form,

$$v_{gas} = v_{kep}\left(1 - \frac{c_s^2}{v_{kep}^2}\right)^{\frac{1}{2}} \tag{2.51}$$

Now, I make the assumption that the correction to the Keplerian velocity is small. That is, $c_s^2 \ll v_{kep}^2$ (for example, in the Solar System at 1 au, c_s is about 1 km/s and v_{kep} is about 30 km/s). I then Taylor expand equation 2.51, giving the approximate expression:

$$v_{gas} = v_{kep}\left(1 - \frac{c_s^2}{2v_{kep}^2}\right) \tag{2.52}$$

$$v_{gas} = v_{kep} - \frac{c_s^2}{2v_{kep}} \tag{2.53}$$

Thus, the orbital velocity of gas in a protoplanetary disk can be easily described using a simple correction to the Keplerian velocity of that gas.

2.5 WISH Radii

I now turn my attention to the basics of how to develop a wind shearing (WISH) radius (from Perets and Murray-Clay, 2011).

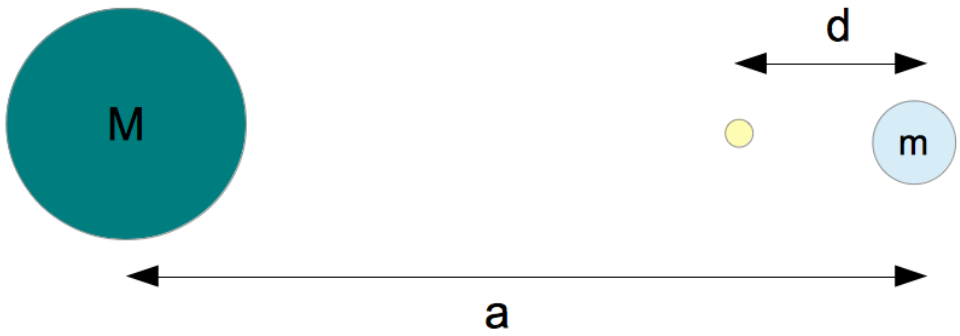

Figure 2.2: Illustration demonstrating distances between the star, the core, and the object

Consider a small object (shown yellow in the diagram), a larger planetary core (shown blue) and a central star (turquoise). The core and the object are in orbit around the star, surrounded by orbiting gas.

In the first scenario (what I label the orbit-capture WISH radius), I consider the object to be orbiting around the central star alone. Therefore, it has some velocity v_{og} relative to the gas, and the core has some other velocity v_{cg} relative to the gas. Each object will have some drag acting on it from the gas, dependent on the area of the cross section of the object (r_{obj}^2 and r_{core}^2, respectively), and on v_{rel}. I represent these differing forces as $F_d(obj)$ and $F_d(core)$. The differing acceleration of each object due to these differing drag forces is given by the equation (from Perets and Murray-Clay, 2011):

$$\Delta a_{ws} = \left| \frac{F_d(object)}{m_{obj}} - \frac{F_d(core)}{m_{core}} \right| \tag{2.54}$$

The WISH radius, then, is the radius at which this differential acceleration (the analog to the gravitational tidal acceleration) overcomes the gravitational attraction to the core, given by the equation:

$$R_{ws} = \sqrt{\frac{G(m_{core} + m_{obj})}{\Delta a_{ws}}} \tag{2.55}$$

For the second scenario (which I label the orbit-maintain WISH radius), I instead assume that the

object is in orbit around the core (like a moon) which is in turn in orbit around the star. In this case, the average velocity with respect to the gas is v_{cg} for both the object and the core. The WISH radius, then, can still be represented by Equation 2.55, but will differ in Δa_{WS} from the previous scenario.

2.6 Understanding Drag Regimes

Next, one must be able to understand how an object placed in the presence of moving gas will act differently from an object in a vacuum. I will now develop a framework to think about the various scenarios of objects in the presence of gas, and the resultant forces.

Depending on the mean free path (λ, given by $\lambda = m_h/\rho\sigma$ where m_h is the mass of hydrogen, ρ is the volumetric density of gas, and σ is the collision cross section between two hydrogen particles), the relative velocity of the object moving through the gas, and the radius of the particle R, different equations are needed to describe the drag force on the object and the differential acceleration between two bodies. The value of λ/R helps to determine which drag regime to use.

2.6.1 $\frac{\lambda}{R} \ll 1$ (Fluid Phase)

In this phase, the mean free path is much smaller than the radius of the particle moving through the gas. Therefore, almost constant collisions are inevitable, and the gas can be thought of as a fluid. In this case, an important number to calculate is the Reynolds number, Re. The Reynolds number is calculated by:

$$Re = \frac{Rv}{\lambda v_{th}} \tag{2.56}$$

where v represents the velocity of the particle and v_{th} represents the thermal velocity of the gas (where $v_{th} \sim c_s$, defined earlier). When $Re \gg 1$, the dynamics of the system are dominated by the object's momentum, and it enters the RAM pressure drag regime. If $Re < 1$, then the dynamics are dominated by the viscosity of the gas, and it enters the Stokes drag regime.

$Re \gg 1$ **(RAM pressure regime)**

Let n represent the number density of the gas, ρ represent the mass density of the gas, and A represent the cross sectional area of a particle. Assuming the gas is made of mostly hydrogen, the change in momentum of the particle per time (the force on the particle) can be represented by the equation:

$$F = (nAv)m_H v \tag{2.57}$$

where nAv is the rate of collisions on the object and m_H is the mass of hydrogen. Thus, the drag force on the object is:

$$F_D = \frac{1}{2}\rho A v^2 \tag{2.58}$$

(gas drag laws reviewed in Batchelor, 1967)

$Re < 1$**(Stokes Drag regime)**

In this phase, one can think of the gas surrounding the object as linearly decreasing from v to 0 as it approaches the object (under a no-slip assumption). The force acting on the side of an object moving in the y direction with area A can be thought of as the difference in velocities just inside and outside it (moving in the x direction), or the shear between the two gases. The momentum of just one gas particle collision, in this case, is $m\,(\delta v_y/\delta x)\,\lambda$, where λ is the mean free path and m is the mass of the gas particle. The force acting on a side of the object with area A is therefore expressed as:

$$F = (nAv_{th})(m_H \frac{\delta v_y}{\delta x}\lambda) \tag{2.59}$$

where the first part is the number of collisions on that side, and the second part is the momentum exchange of each collision. Furthermore, the scale of transition (of the gas) from v to 0 is about

the same scale as the size of the particle. Therefore, I can estimate:

$$\frac{\delta v_y}{\delta x} \propto \frac{v}{R} \tag{2.60}$$

Thus, plugging in, I get that:

$$F_D \propto nR^2 v_{th} m_H (\frac{v}{R})\lambda \tag{2.61}$$

$$\propto \rho R \lambda v v_{th} \tag{2.62}$$

This is kinematic viscosity. Let $\nu = v_{th}\lambda$. Furthermore, let η represent $\rho\nu = \rho v_{th}\lambda$. Thus, I arrive at the drag force:

$$F_D = 6\pi\eta R v \tag{2.63}$$

(Stoke's Law developed by George Stokes in 1851, drag laws reviewed in Batchelor, 1967).

2.6.2 $\frac{\lambda}{R} > 1$ (Diffuse Phase)

In this regime, an important number for classification is the Mach number, M. The Mach number is defined as:

$$M = \frac{v}{c_s} \tag{2.64}$$

where v is the velocity of the object and c_s is the speed of sound in that gas. If $M < 1$, then the object is relatively slow-moving, and is bombarded with particles from all sides. This is called the Epstein drag region. If $M > 1$, then the object is moving fast enough that gas particles coming at it from behind are not fast enough to catch up, so the object only collides with gas particles in front of it. This region is identical to the RAM pressure drag region.

$M < 1$ (Epstein Drag regime)

For this regime, I move to a reference frame in which the object is stationary. Particles bouncing off the top and bottom of the object are equal in number, so the forces in that direction cancel out.

In the front of the particle, however, objects collide with velocity $v + v_{th}$, and in the back, with velocity $v_{th} - v$. The drag force the object feels is the front force minus the back force. One can write each as:

$$F_{d(front)} = nAm(v_{th} + v)^2 \tag{2.65}$$

$$F_{d(back)} = nAm(v_{th} - v)^2 \tag{2.66}$$

Where the momentum exchanged is $m(v+v_{th})$ and $m(v_{th}-v)$, respectively, and the rate of collision is $nA(v + v_{th})$ and $nA(v_{th} - v)$, respectively. Thus, the total drag force felt is:

$$F_D \propto \rho A[(v_{th} + v)^2 - (v_{th} - v)^2] \tag{2.67}$$

$$F_D \propto \rho A v v_{th} \tag{2.68}$$

$M > 1$ **(RAM pressure regime)**

In this regime, the dynamics are the same as in the momentum-dominated fluid phase. Therefore the drag force is the same equation:

$$F_D = \frac{1}{2}\rho v^2 R^2 \tag{2.69}$$

Using these 4 regimes, I can model the behavior of an object moving through gaseous protoplanetary disks.

2.7 Understanding Particle Capture in the Presence of Gas

Now I have the tools needed to understand the difference between accretion in a vacuum and accretion in the presence of gas. I apply the physics from this chapter to develop a framework of testing whether a particle will accrete onto a core or not. In this section, I develop an intuition for imagining the possible trajectories of different particles. I further develop a simple framework for testing whether a particle will accrete, without having to rely on solving explicitly for the particles complete path of motion.

A particle will orbit with different velocities, depending not only on its distance to the star,

but also because of the drag force due to the slower-orbiting gaseous environment. Objects are affected differently depending on their size and mass, as both cross-sectional contact with the gas and inertial momentum are affected.

In order to determine whether a certain sized object will accrete onto the planetary core, I set up a simple system, whereby an object, traveling at velocity v_{obj}, travels in a straight line towards a core (traveling at velocity v_{core}). The entire system is encased in a gas traveling at velocity v_{gas}. I assume that the planetary core is large enough that its velocity is not significantly affected by gas drag on the timescale of its encounter with the approaching object. I then set certain conditions to put constraints on the object's ability to spiral into the core.

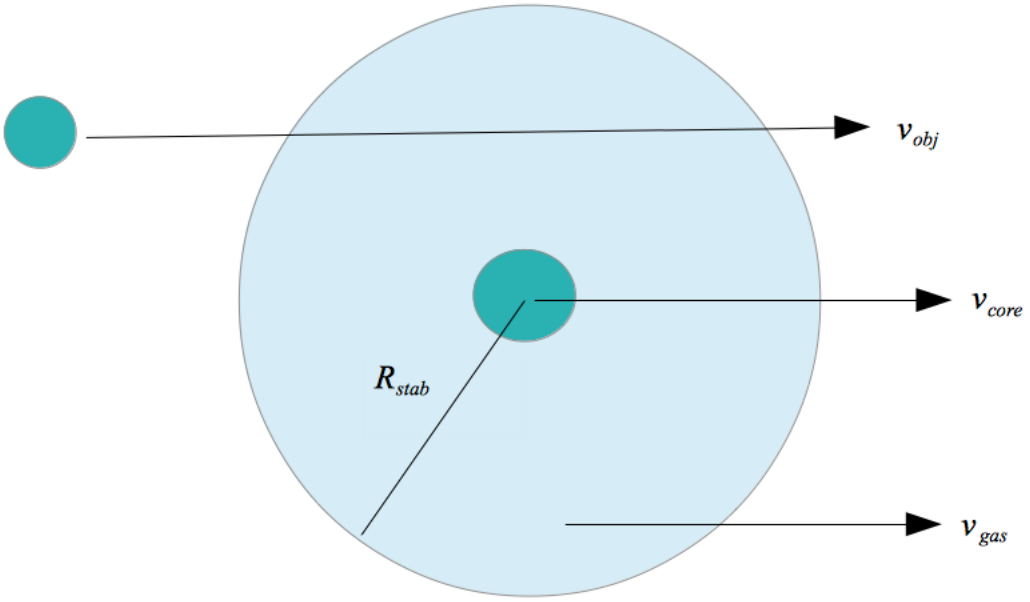

To begin, I define certain parameters. The important velocities in the problem are not the proper motions of the components themselves, but rather their relative velocities to one another. Thus, I define:

$$v_{og} = |v_{obj} - v_{gas}| \tag{2.70}$$

$$v_{oc} = |v_{obj} - v_{core}| \tag{2.71}$$

$$v_{cg} = |v_{core} - v_{gas}| \tag{2.72}$$

2.7.1 Stable Radius

The first condition concerns the distance of the object at its closest point to the core. In previous discussion, I have defined a radius, either the Hill radius or the WISH radius, that constitutes the maximum radius of orbit of a bound system. Beyond this, the object will either be gravitationally pulled away by the influence of the star, or it will be sheared away by gas interaction.

Thus, I plug in the parameters for the radius of stability for the core, as a function of the mass of the core, its distance from the star, and its relative velocity with the gas, v_{cg}. This gives the maximum cross section of collisions for the planetesimal.

2.7.2 Energy Constraints

The second condition concerns the energy of the incoming particle. As the particle approaches the core's stable radius, it is acted upon by a drag force from the gas. This drag force does work on the particle, which then reduces its energy. As the particle dissipates energy, it slows down. Eventually, the particle will have lost an amount of energy equal to its initial kinetic energy relative to the core. At that point, the particle will be gravitationally bound to the core, and will eventually spiral in and accrete onto the core.

There are two regimes that are intuitively important in thinking about the energy dissipation of the object. They are defined by the relative size of the Bondi radius to the stable radius of the core. Consider the motion of gas around a rigid spherical body, as simulated by Ormel in Figure 5 of his paper (Ormel, 2013):

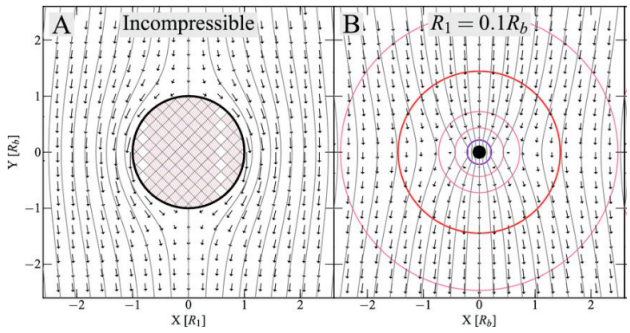

Figure 2.3: 2D cross-section of simulated gas flow around a rigid body. Taken from Ormel, 2013, Figure 5.

In reality, the gas is compressible rather than incompressible, so Figure 2.3(b) is a more correct

diagram than 2.3(a). I will approximate the core to be rigid for the purposes of this paper, however. The relevant length scale here is R_{bondi}. The bondi radius is given by:

$$R_{bondi} = \frac{GM_{core}}{{c_s}^2} \tag{2.73}$$

And comes from equating the relative velocity of a gas molecule (v_{cg}) to the escape velocity of the core – essentially the gas binding distance of the core. This represents the maximum radius at which gas particles are considered part of the core's atmosphere, or, referring to the figure, where the gas particles are significantly bent off-course. I can make two descriptive pictures of the core-object interaction, shown below in Figure 2.4:

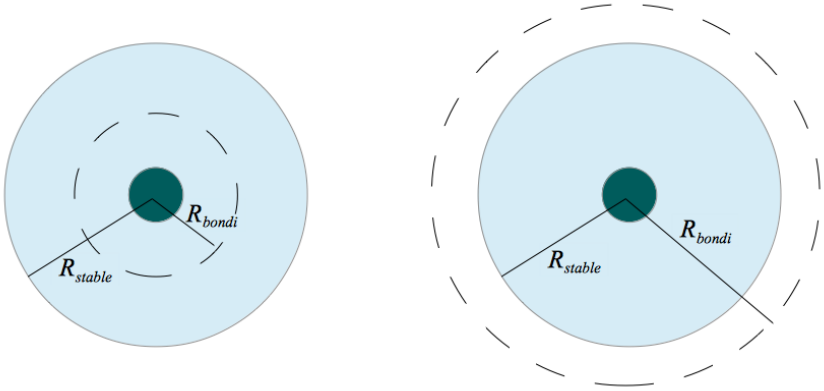

Figure 2.4: Depiction of possible relationships between stable radius and Bondi radius. For small approaching particles dominated by the WISH radius constraint, the relationship on the right is appropriate. For larger particles, the left is appropriate.

On the left side, the stable radius of the core is larger than the Bondi radius. In this case, the incoming particle, in order to spiral into the core and accrete, must dissipate all its kinetic energy (relative to the core) by the time it crosses the stable radius.

On the right side, however, the Bondi radius of the core is larger than the stable radius. In this case, in order for the particle to be caught within the stable radius, it must first enter the Bondi radius. If it has dissipated all its kinetic energy and coupled to the gas, then it will not be able to enter the Bondi radius – it will simply flow around the core without accreting. Thus, in order for the particle to accrete in this instance, it must not dissipate all its kinetic energy relative to the

core over the length scale of the Bondi radius. The following condition must hold:

$$\text{If } R_{bondi} \leq R_{stable},\ F_D R_{stable} \geq \frac{1}{2} m_{obj} v_\infty^2 \tag{2.74}$$

$$\text{If } R_{bondi} \geq R_{stable},\ F_D R_{bondi} \leq \frac{1}{2} m_{obj} v_\infty^2 \tag{2.75}$$

2.8 Velocity Adjustment During Encounters

One also must look at what happens to the kinetic energy – and therefore velocity – of a test particle as it encounters the planetary core. Consider the following diagram:

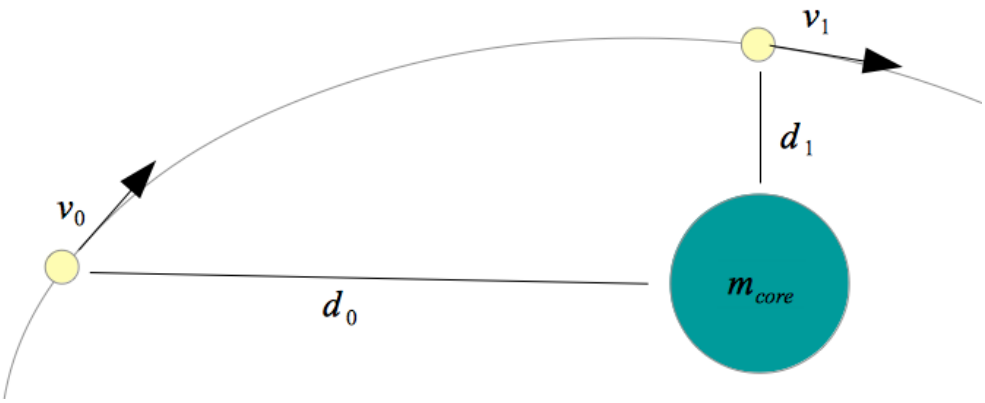

Figure 2.5: Diagram showing velocity adjustment during a particle-core encounter.

I set 0 potential energy to be at a distance of ∞ from a core with mass m_{core}. Furthermore, I assume that the test particle has mass m_{obj}.

At location d_0, the test particle's total energy is:

$$E = \frac{1}{2} m_{obj} {v_0}^2 - \frac{G m_{core} m_{obj}}{d_0} \tag{2.76}$$

At location d_1, the test particle's total energy is:

$$E = \frac{1}{2} m_{obj} {v_1}^2 - \frac{G m_{core} m_{obj}}{d_1} \tag{2.77}$$

Total energy is conserved, so equating the two energy expressions and taking out the mass depen-

dence yields:

$$\frac{1}{2}{v_0}^2 - \frac{Gm_{core}}{d_0} = \frac{1}{2}{v_1}^2 - \frac{Gm_{core}}{d_1} \tag{2.78}$$

One can assume that d_0 is much larger than d_1 (since, at some point, the test particle was very far away from the core. Thus, the term $Gm_{core}/d_0 \to 0$.

If v_0 is very small in comparison to v_1, then this too is approximately 0, and therefore:

$$v_1 \approx \sqrt{\frac{Gm_{core}}{d_1}} \tag{2.79}$$

Thus, if a particle is moving at a velocity slow compared to the orbit velocity at the stable radius of the core, by the time of its encounter with the core, it will be moving at approximately a velocity that corresponds to the orbital velocity at the stable radius, or the "stable velocity."

2.9 A Note on Geometry

In the model, I take geometry into account when I determine the velocity of the accreting particle, by calculating the components of its velocity in the radial and orbital directions. This will give a sense of how to incorporate geometry into the relative motion between the planetesimal and the planetary core.

On the other hand, however, I have not taken into account geometry with respect to gas flow. The following diagram, for instance, shows a possible picture (from the perspective of the planetary core):

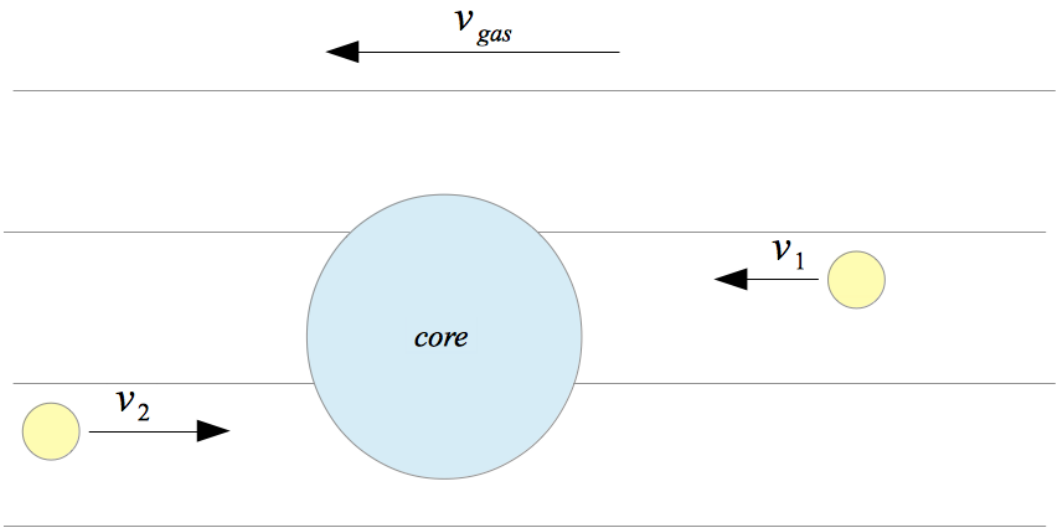

Figure 2.6: Diagram showing one of the geometrical intricacies of gas interaction.

Both of these particles, 1 and 2, will collide into the planetary core. In the frame of the core, both particles are moving towards it. In the frame of the gas, however, the geometry is different. Particle 1, moving at velocity $v1$, is moving towards the planet, but the drag force from the gas is working against it. Particle 2, on the other hand, is moving towards the planet, but the gas drag works to speed the particle up, not slow it down.

In my simulation, depending on the velocities, I would not be able to distinguish between these two scenarios. I simply calculate the relative velocity between the object and the gas, not knowing whether the gas is working to slow it down or speed it up. Of course, however, the accretion probability is different between the two particles.

Thus, in fact, for half the particles tested, I do not know the exact geometry of the encounter and may not be able to predict the accretion probability. This geometry correction would be a good place to start doing further research. On the other hand, at worst, I can assume that any particle that I have incorrectly modeled will not be able to accrete. This would mean that, at worst, the accretion mass is half what I originally thought, and the timescale of growth will therefore be double. This is a correction only on the order of unity, which is insignificant compared to the order of magnitude of reductions I make to the gravitational focusing timescales. This is an important point to consider going forward with the model, as well as for future work.

Chapter 3

Creating the Model

3.1 Preliminaries

Now I construct a model that can predict the growth timescale for a core in disk conditions. First, I define some constants in the units that are used in the model (cgs units).

3.1.1 Constants

I define certain constants as such:

$$G = 6.674 \times 10^{-8} \frac{cm^3}{g * s^2} \text{ (Gravitational Constant)}$$

$$\pi = 3.1416$$

$$k = 1.381 \times 10^{-16} \frac{erg}{K} \text{ (Boltzmann Constant)}$$

$$\mu = 3.85 \times 10^{-24} g \text{ (mean molecular weight of a particle)}$$

$$AU = 1.496 \times 10^{13} cm \text{ (Astronomical Unit)}$$

$$\sigma = 10^{-15} cm \text{ (the neutral collision cross-section of protoplanetary disk gas)}$$

3.1.2 Assumptions

Furthermore, I make several assumptions about the protoplanetary system. The following values can be changed depending on the nature of the system in question, and will provide all the raw

information needed to predict protoplanetary growth:

a_{core} = distance to star from core in au

ρ_{p} = density of bodies in g/cm^3

M_* = mass of star in g

m_{core} = starting mass of core in g

m_{obj} = mass of accreting objects (I assume all accreting objects are a constant size)

r_{core} = starting radius of core in cm

r_{obj} = radius of accreting objects

$\Sigma(a)$ = surface density of disk in g/cm^2 – a function

T(a) = temperature of system in Kelvins – a function

$f_{accrete}$ = the fraction of disk mass made of accretable material (dust to gas ratio)

where, of course, either the mass of the core/planetesimal or the radii of the two is needed, but not both (using the density of bodies, one can easily relate the two by $m = \frac{4}{3}\pi r^3 * \rho_p$). For the sake of this chapter, I demonstrate the flow of the model using solar system masses an example. I consider the planetary core to be Earth mass and radius (5.97×10^{27} g in mass, 6.37×10^8 cm in radius), the star to be Sun-size (1.9891×10^{33} g in mass) and the distance between the two bodies to be 10 AU. While I will explore a range of test particle sizes, the numbers listed will be for test particles 10 cm in radius, with a density of $2g/cm^3$. I assume disk surface density Σ and temperature profiles of:

$$\Sigma = 2 \times 10^3 \left(\frac{a_{core}}{AU}\right)^{-1} \tag{3.1}$$

$$T = 120 \left(\frac{a_{core}}{AU}\right)^{-\frac{3}{7}} \tag{3.2}$$

Finally, I assume that the protoplanetary disk is a laminar disk. That is to say, the gas flows in an orbit around the star with no turbulence.

3.1.3 Equations

From here, I combine the assumed values and constants to calculate some basic quantities that will be useful later on in the model. First, I calculate the Keplerian orbital frequency of the core, :

$$\Omega = \sqrt{\frac{GM_*}{a_{core}^3}} \tag{3.3}$$

(In the example, $\Omega = 6.30 \times 10^{-9}\text{s}^{-1}$)

Next, I calculate the speed of sound in the disk:

$$c_s = \sqrt{\frac{kT}{\mu}}\text{cm/s} \tag{3.4}$$

(In the example, $c_s = 4.0 \times 10^4$ cm/s)

From this, I calculate the density of the gas in the disk. The disk scale height can be represented by:

$$H \sim \frac{c_s}{\Omega} \tag{3.5}$$

(in the example, $H = 6.36 \times 10^{12}$ cm)

From this I arrive at the relation for gas volume density, :

$$\rho_g \sim \frac{\Sigma}{2H} \tag{3.6}$$

($\rho_g = 1.57 \times 10^{-11}$ g/cm^3)

Combining these values together, one can arrive at the mean free path of the gas in the protoplanetary disk(λ), given by:

$$\lambda = \frac{\mu}{\rho_g \sigma} \tag{3.7}$$

($\lambda = 245$ cm)

The thermal velocity of the gas (v_{th}) can be given by:

$$v_{th} = \sqrt{\frac{8}{\pi}} c_s \tag{3.8}$$

($v_{th} = 6.39 \times 10^4$ cm/s)

And with these values now calculated, I start the modeling.

Model framework

The basic framework of the model is such. I choose a test particle of size m_{obj}, located at a distance a_{obj} from the star. I model the effect of pressure on the gas to get a realistic estimate for the average velocity of the gas at that distance. Next, by determining the gas drag regime of the test particle in the gas, I apply the appropriate drag laws to get an accurate picture of the real velocity of that particle (before it encounters the planetary core).

Next, I use what I know about the core, the particle, and their relationship to calculate the energy of the particle at ∞ and the energy dissipation due to gas drag (see section "Understanding Particle Capture in the Presence of Gas" for an explanation of the relevant values). If the correct relations hold to guarantee accretion of the particle, then I add this "test location" (a distance d from the core) to the capture area. If not all the correct relations hold, then I omit this from the capture area.

Timescales

By running this series of steps for sufficient test particles (at different distances d from the core) then I create an effective capture radius for a specific core in specific protoplanetary conditions (counting only those distances that accrete). After that, I use the simple equation below to determine the timescale of growth of the core:

$$\text{timescale} = \frac{m_{core} H}{\Sigma A_{accrete} v_{oc}} \tag{3.9}$$

where H is the scale height of the disk, Σ represents the surface density of the disk, $A_{accrete}$ represents the area of accretion, and v_{oc} represents the relative velocity between the core and the particles it is accreting. In the gravitational focusing case, when no gas disk is assumed, the timescale is instead given by:

$$\text{timescale} = \frac{m_{core}}{A_{accrete}\Sigma\Omega} \tag{3.10}$$

(This can be derived by setting $v_{oc} = v_{rand}$ and $H = v_{rand}/\Omega$, using the random velocity discussion from Chapter 2.2). If the timescale of growth is less than the typical lifespan of protoplanetary disks of those characteristics, then it is possible for the core of a gas giant to have formed through accretion mechanisms at that location in the system.

3.2 Model

3.2.1 Determining Stable Radius

First I must determine whether the test particle falls within the radius of stability of the core. There are three criteria for this: first, the particle at its present location must be able to be captured into a stable radius without being sheared away by gas (thus we envision the particle as in orbit around the star). Second, the particle, once in orbit, must be able to stay there (and cannot be sheared away by gas from its new orbital location) – thus I envision the particle as in orbit around the core, and the particle-core system as a whole in orbit around the star. Third, the particle must not be sheared away by gravitational tidal forces due to the central star. I therefore determine the stable radius in three separate ways: R_{ws}(Orbit Capture), R_{ws}(Orbit Maintain), and R_{Hill}. I use the smallest of the three as the conservative standard.

Hill Radius

First I determine the Hill Radius for the core (for a deeper discussion of the Hill radius, see the Hill radius derivation in the derivations section). The Hill radius is given by:

$$R_{Hill} = a_{core}\left(\frac{m_{core}}{3M_*}\right)^{\frac{1}{3}} \tag{3.11}$$

($R_{Hill} = 1.50 \times 10^{12}$ cm)

Orbit Capture WISH Radius

In order to find the orbit capture WISH radius, I first determine the terminal velocity of the test particle. Then, I use this to find the tidal acceleration due to gas forces (between the test object and the core) and from that I derive a radius of stability.

The orbital velocity of the core is given by:

$$v_{core} = \sqrt{\frac{GM_*}{a_{core}}} \tag{3.12}$$

($v_{core} = 9.42 \times 10^5$ cm/s)
At the distances I am dealing with (along the scale of R_{Hill}) the Keplerian orbital velocity of the test particle can be estimated to be the same as the core, v_{core} (since d, the distance between the core and the test particle, satisfies $d \leq R_{Hill}$, $d \ll a_{core}$). Thus I set $v_{obj} = v_{core}$
($v_{obj} = 9.42 \times 10^5$ cm/s)

I define the orbital velocity of the gas around the planetary core to be the Keplerian velocity, adjusted to account for gas pressure (for explanation of adjustment, see previous section):

$$v_{gas} = v_{core} - \frac{c_s^2}{2v_{core}} \tag{3.13}$$

($v_{gas} = 9.41 \times 10^5$ cm/s)
Now, to see how the velocity of the test particle will change because of the presence of gas, I first

need the relative velocity between the test particle and the gas:

$$v_{rel} = v_{obj} - v_{gas} \tag{3.14}$$

I now find the Reynolds number and drag constant for the test particle, according to the following equations:

$$Re_{obj} = \frac{2 r_{obj} v_{rel}}{.5 v_{th} \lambda} \tag{3.15}$$

$$c_{d_{obj}} = \frac{24}{Re_{obj}} \left(1 + 0.27 Re_{obj}\right)^{0.43} + 0.47 \left(1 - e^{-.04 Re_{obj}^{0.38}}\right) \tag{3.16}$$

Now I apply drag force laws to adjust the velocity of the test particle. If the particle is in the Stokes or RAM pressure regime, I use the smoothed drag force equation given by Cheng, 2009:

$$F_d = \frac{1}{2} c_d \pi r_{obj}^2 \rho_g v_{rel}^2 \tag{3.17}$$

If the particle falls in the Epstein regime (defined by $r_{obj} \geq 9\lambda/4$), however, Cheng 2009 does not hold. Instead, I use the Epstein-specific drag force law, given by:

$$F_D = \frac{4}{3} \pi \rho_g v_{th} v_{rel} r_{obj}^2 \tag{3.18}$$

For the knowledge of how this drag force will affect both the radial and orbital components of the velocity, I refer to Perets and Murray-Clay, 2011. First, I define the constants η, t_s, and v_{kep} to be:

$$v_{kep} = \sqrt{\frac{G M_{star}}{a_{core}}} \tag{3.19}$$

$$\eta = 0.5 \left(\frac{{c_s}^2}{{v_k}^2}\right) \tag{3.20}$$

$$t_s = \frac{m_{obj} v_{rel}}{F_d} \tag{3.21}$$

where t_s represents the stopping time of a particle at that velocity and v_{kep} is the Keplerian velocity of a particle at that distance. Next, I use the two formulas below to calculate the new radial and

orbital velocities:

$$v_{rel,r} = -2\eta v_{kep}[\frac{t_s\Omega}{1+(t_s\Omega)^2}] \tag{3.22}$$

$$v_{rel,\phi} = -\eta v_{kep}[\frac{1}{1+(t_s\Omega)^2} - 1] \tag{3.23}$$

where $v_{rel,r}$ represents the velocity component towards/away from the star and $v_{rel,\phi}$ represents the velocity component in the orbital direction. From here, the relative velocity is now set to be:

$$v_{rel} = \sqrt{v_{rel,r}^2 + v_{rel,\phi}^2} \tag{3.24}$$

I repeat this process (starting with finding the Reynolds number and drag constant) again and again, until v_{rel} does not change. At this point, I have determined the terminal velocity of the particle in the gaseous disk (before encountering the core).

I then define the following relative velocities:

$$v_{obj,r} = v_{rel,r} \tag{3.25}$$

$$v_{obj,\phi} = |v_{rel,\phi} + v_{gas}| \tag{3.26}$$

$$v_{cg} = |v_{core} - v_{gas}| \text{ (relative velocity between core and gas)} \tag{3.27}$$

$$v_{og} = v_{rel} \text{ (relative velocity between test particle and gas)} \tag{3.28}$$

$$v_{oc} = \sqrt{|v_{obj,\phi} - v_{core}|^2 + v_{obj,r}^2} \text{ (relative velocity between test particle and core)} \tag{3.29}$$

($v_{obj,r} = 384$ cm/s, $v_{obj,\phi} = 9.41 \times 10^5$ cm/s, $v_{cg} = 851$ cm/s, $v_{og} = 211$ cm/s, $v_{oc} = 864$ cm/s)

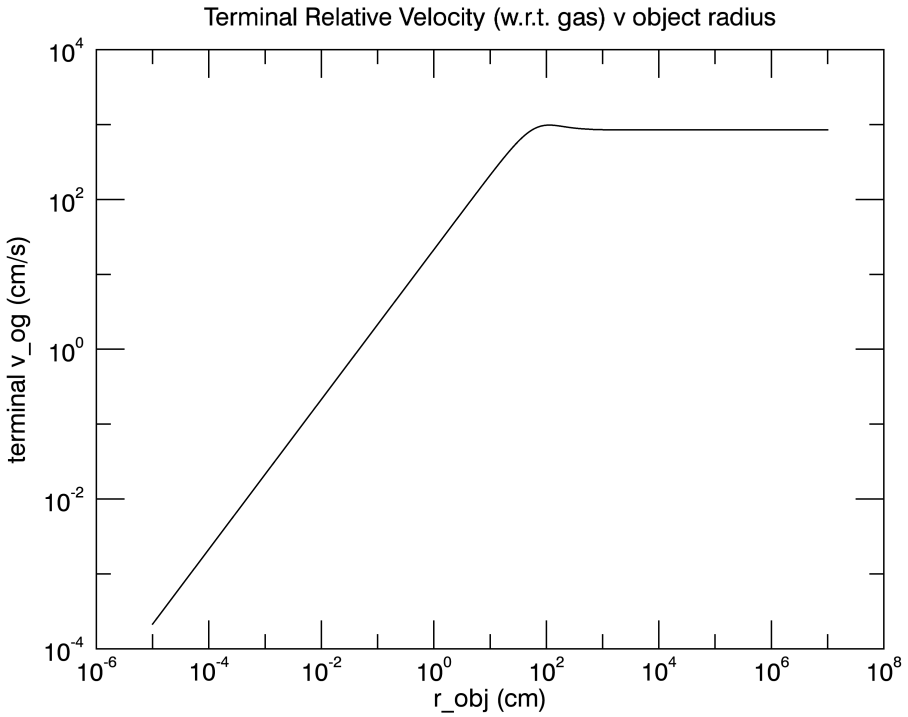

(a) Relative terminal velocity of test particle with respect to gas. Changing the radius of the particle affects the force of the drag on the particle, which changes the terminal velocity of the particle.

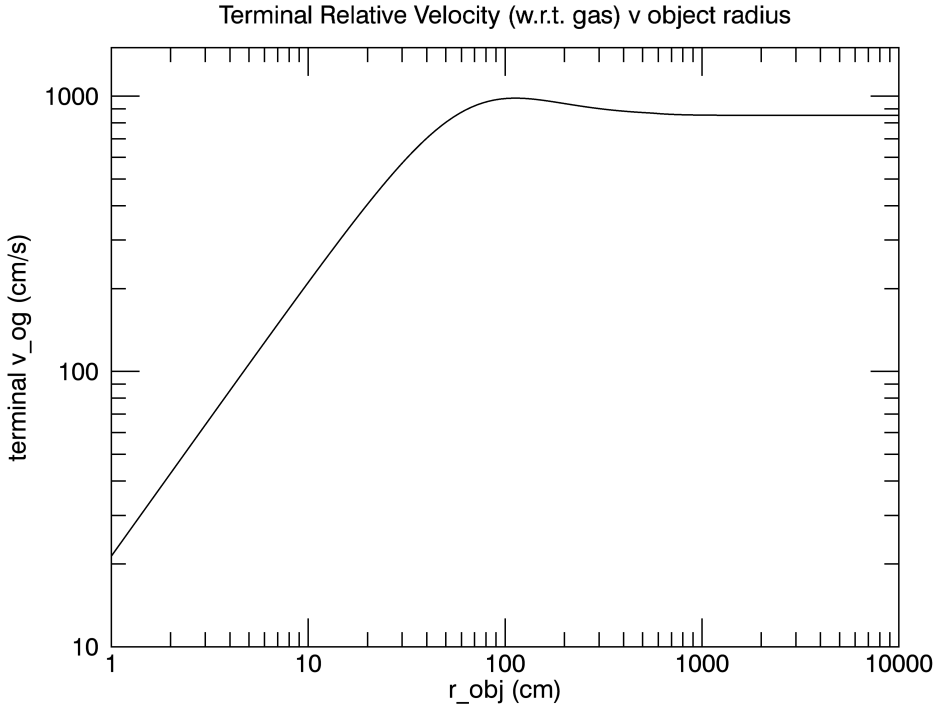

(b) Graph showing peak of relative terminal velocity. Peak is at about 100cm, illustrating the "meter barrier" problem.

Figure 3.1: Relationship between terminal velocity relative to the gas velocity and test particle size (radius).

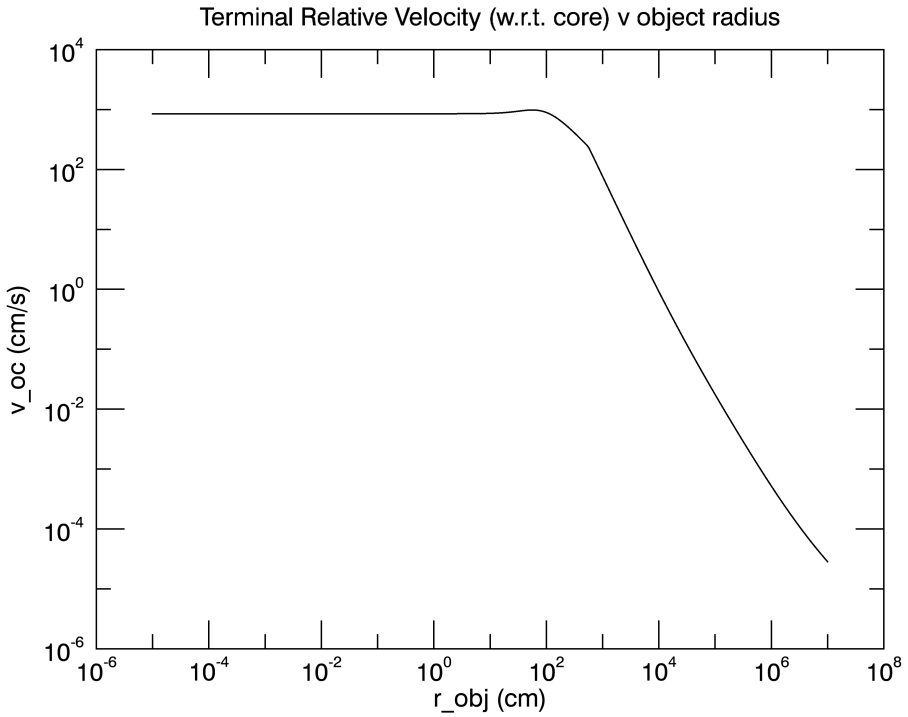

(a) Relative terminal velocity between the test object and the core. This relative velocity will be important in determining whether the particle is moving at the right speed to accrete onto the core, as well as help to determine the WISH radius of the core.

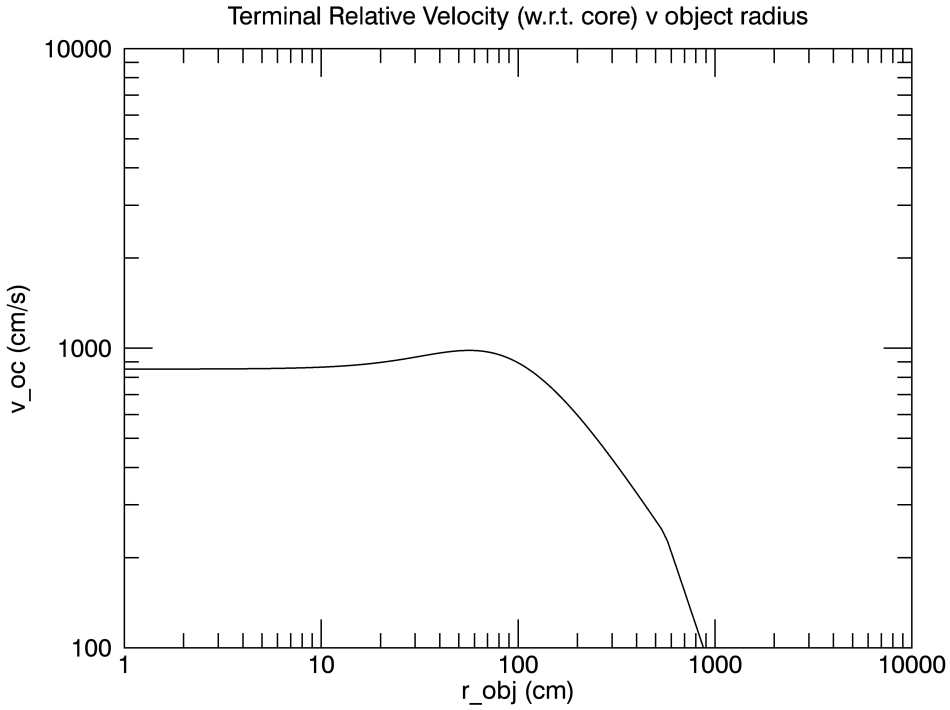

(b) Zoomed in view of peak relative velocity between object and core.

Figure 3.2: Relationship between terminal velocity of a test object relative to the velocity of the core and the test object's size (radius).

I now find the Reynolds number and drag constant for both the core and the test particle according to the equations from earlier in the chapter. I use v_{cg} for v_{rel}, r_{core} for r in the case of the core and v_{og} for v_{rel}, r_{obj} for r in the case of the object. ($Re_{core} = 1.39 \times 10^5$, $Re_{obj} = 5.38 \times 10^{-4}$, $c_{d_{core}} = 0.473$, $c_{d_{obj}} = 4.46 \times 10^4$)

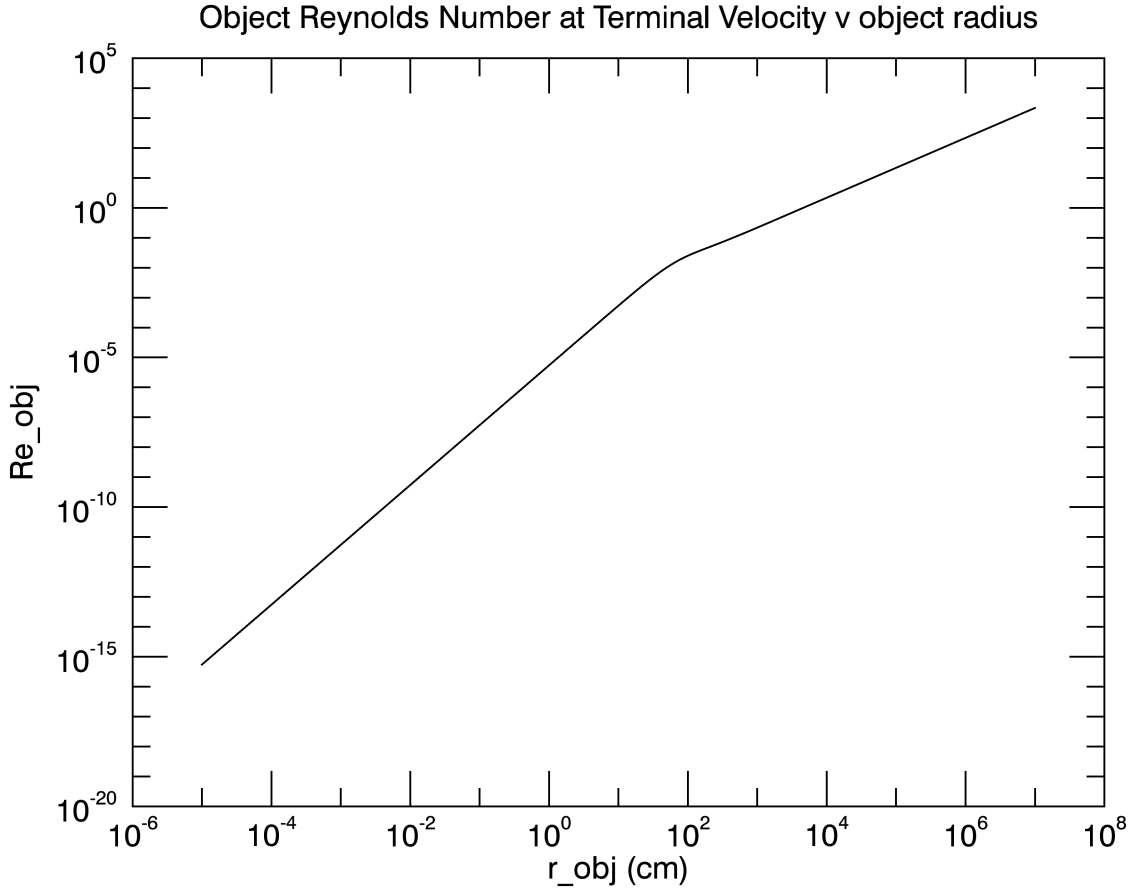

Figure 3.3: Re_{obj} at terminal velocity. The plot shows a clear break at about 100 cm corresponding to the transition between the Stokes and Epstein regimes.

I now use the appropriate drag force equation (either Cheng, 2009, or the general Epstein regime equation, depending on the radius of the particle) to calculate the drag force experienced by the core and the test particle (Brown & Lawler, 2003; Cheng, 2009): ($F_{d_{core}} = 1.46 \times 10^{15}$ dynes, $F_{d_{obj}} = 8.86 \times 10^{-2}$ dynes)

where v_{rel} is the relative velocity w.r.t. the gas (v_{og} for the test particle, v_{cg} for the core).

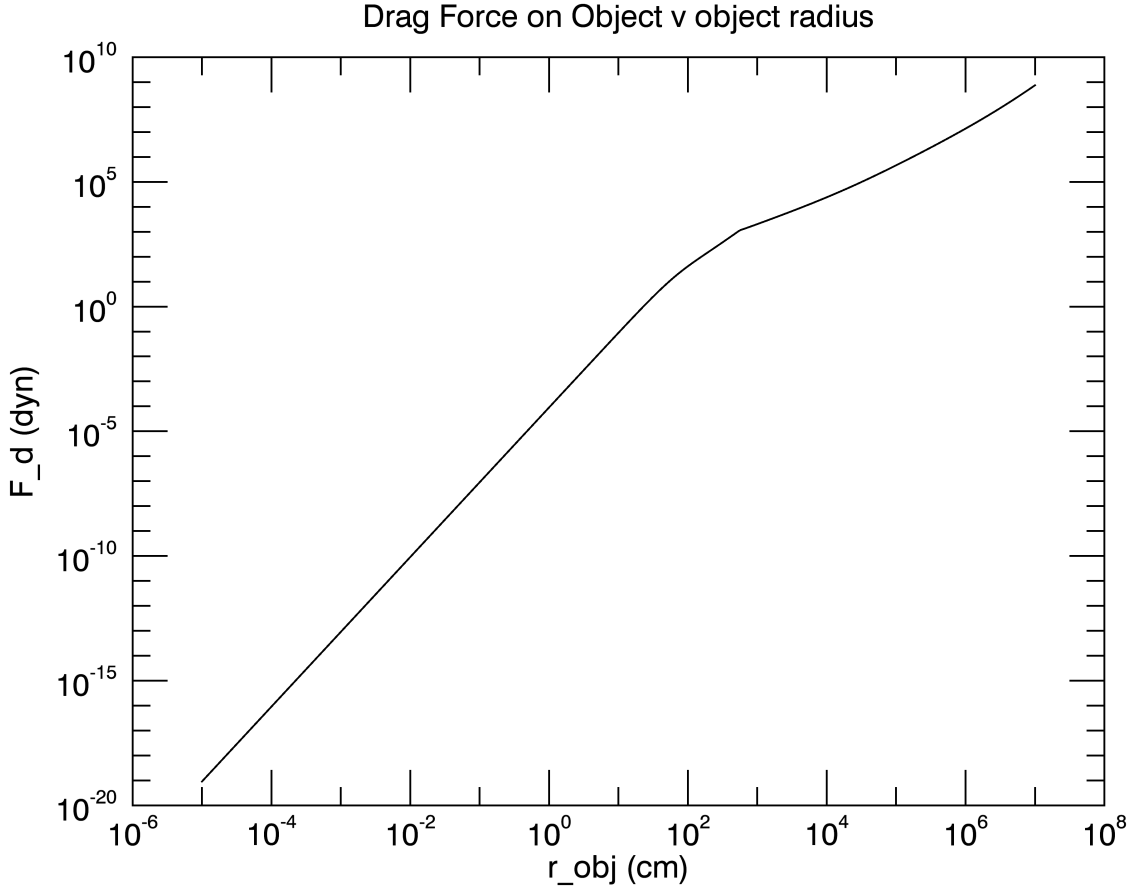

Figure 3.4: $F_{d_{obj}}$ relative to particle size. As particles get smaller, their terminal velocities are closer and closer to the velocity of the gas. Thus, the lower limit on the drag force would be the force required to keep a particle at the gas's orbital velocity (below the Keplerian velocity of object).

I then use these drag forces to find the differential acceleration between the particle and the core due to drag, or wind shearing, by using the equation:

$$\Delta a_{WS} = \left| \frac{F_d(\text{object})}{m_{obj}} - \frac{F_d(\text{core})}{m_{core}} \right| \tag{3.30}$$

($\Delta a_{WS} = 1.06 \times 10^{-5}$)

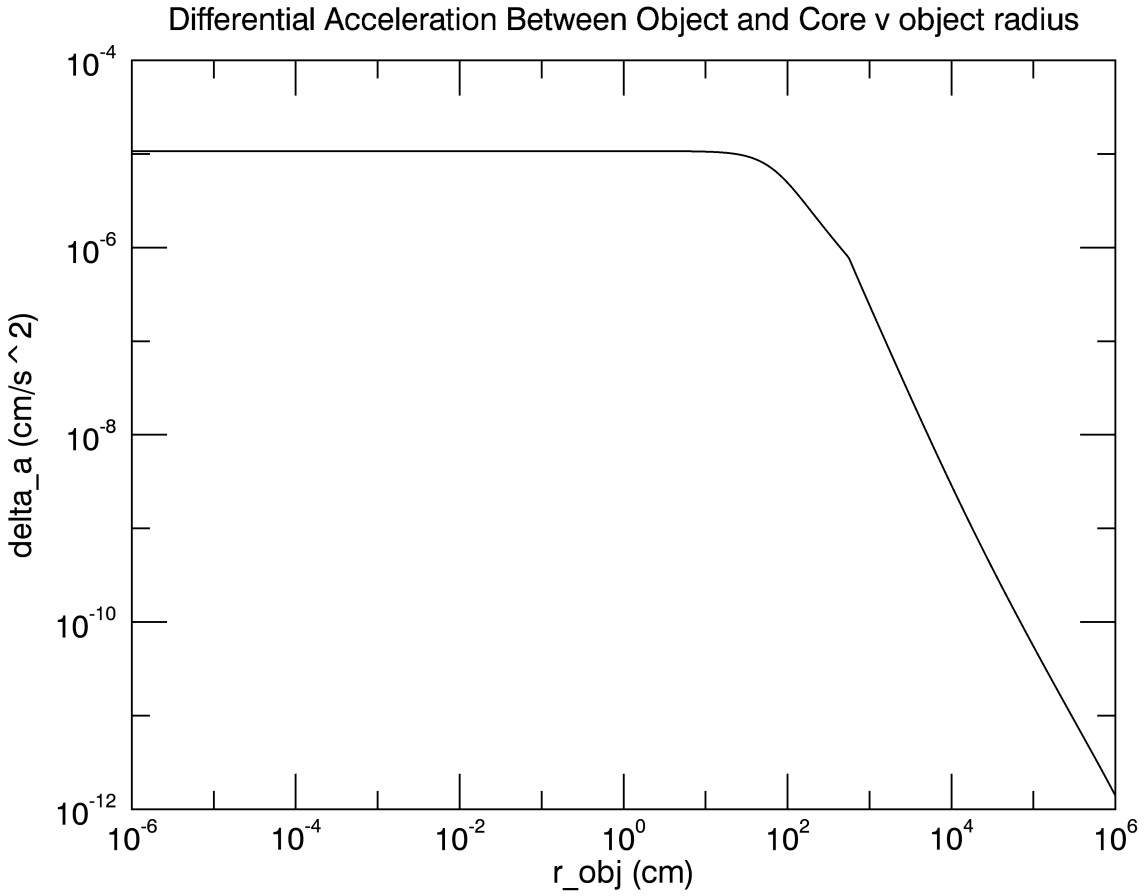

Figure 3.5: Δa_{WS} compared to radius of test particle. This differential acceleration serves the same purpose as differential acceleration due to gravitational tidal forces serves in determining the Hill radius.

I define the wind shearing radius, or the WISH radius, to be the distance between the two objects where the differential acceleration between the two due to drag overcomes the gravitational attraction between the two. Thus, the orbit capture WISH radius is:

$$R_{WS} = \sqrt{\frac{G(m_{core} + m_{obj})}{\Delta a_{WS}}} \tag{3.31}$$

($R_{WS} = 6.14 \times 10^{12}$ cm)

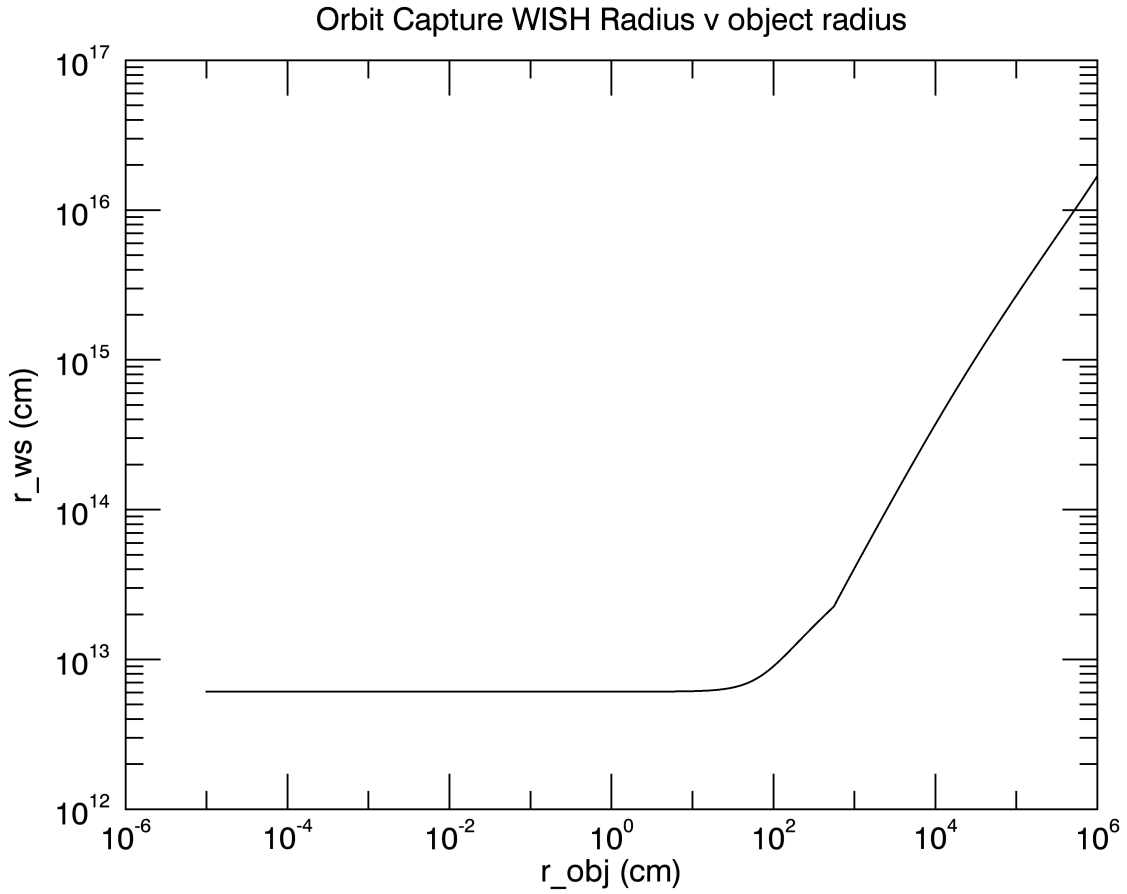

Figure 3.6: Comparing the orbit-capture WISH radius to r_{obj}. In the orbit capture scenario, I consider the particle to be in orbit around the central star (instead of around the core). I then calculate, based on the relative velocity of the particle with respect to the gas, the radius at which wind-shearing prevents the particle from entering into orbit around the core. A particle that lies outside this WISH radius experiences such shearing forces from the gas that it is pulled away by the gas, instead of slowed down to an orbit-acceptable velocity.

Orbit Maintain WISH Radius

To find the WISH radius assuming the particle is already in orbit around the core, I follow a similar procedure. I use the same Reynolds numbers and drag constants (for the planet core) found in the previous section. v_{rel} does not change for the core (I still use v_{cg} as the value). However, I now assume that the test particle is already in orbit around the core, rather than the star (see Chapter 2.5). Thus, the relative velocity between the gas and the particle, averaged around the particle's orbit, is the same as the relative velocity of the core, v_{cg}.

I thus recalculate the Reynolds number of the test particle, the drag constant, and finally the drag force on the test particle, and from there recalculate the differential acceleration. Plugging in this new Δa_{WS} to the equation for WISH Radius, I arrive at a value for the orbit maintain WISH Radius.

($F_{d_{core}} = 1.46 \times 10^{15}$, $F_{d_{obj}} = 0.36$, $\Delta a_{WS} = 4.28 \times 10^{-5}$)

($R_{WS} = 3.05 \times 10^{12}$ cm)

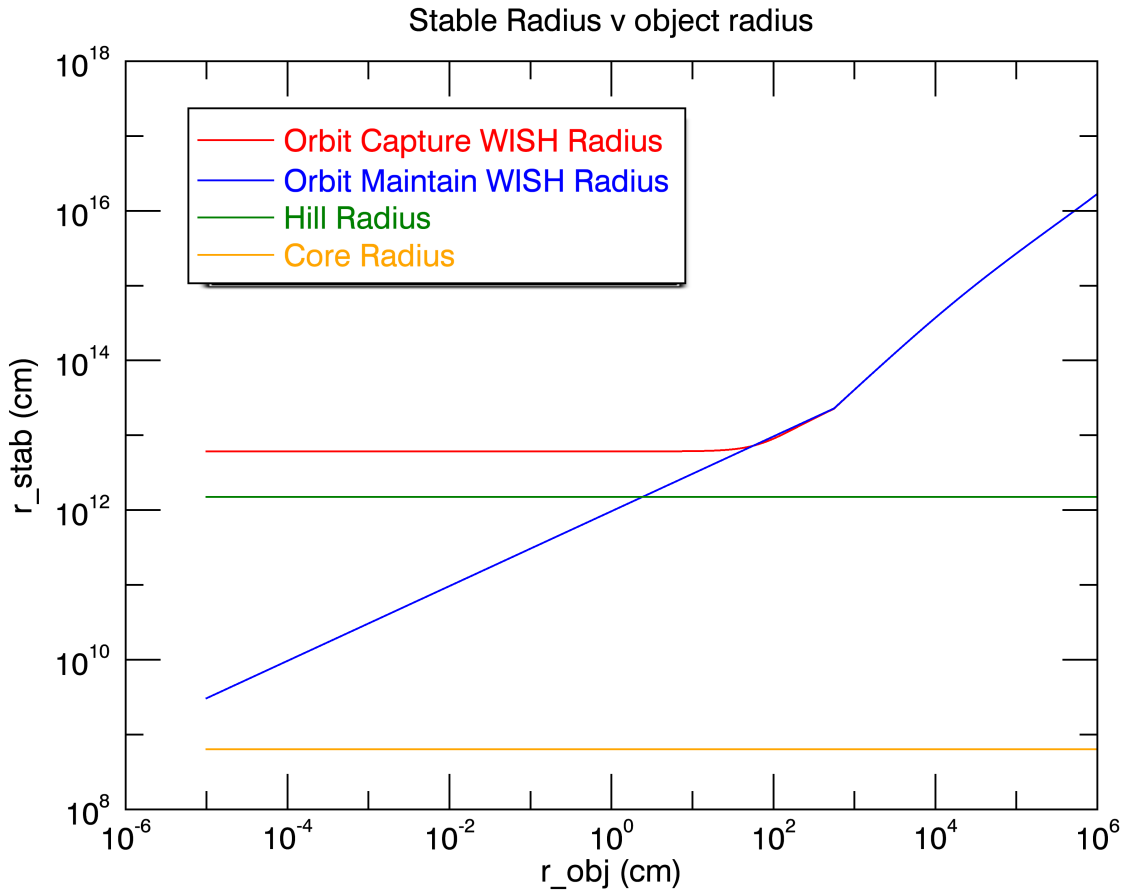

Figure 3.7: Graph comparing the three radii found using the example numbers. In green is the Hill radius, the point (in a gas-free environment) at which the particle will be pulled away from orbit around the core by tidal forces from the central star. In red is the WISH radius for the orbit-capture technique, explained earlier in this chapter. In blue is the orbit maintain WISH radius, the radius at which a particle in orbit around the planetary core will be sheared away by differential gas acceleration between the two objects. In orange is the radius of the core. For small sizes of particles, the Orbit Maintain WISH radius is the smallest of the three stable radii, but for most sizes, the Hill radius is the smallest stable radius, and the limiting factor in a particle's ability to enter into orbit around the core.

Choosing the Stable Radius

I now have three possible values for the stable radius of the core: R_{ws}(orbit capture), R_{ws}(orbit maintain), and R_{Hill}. I choose the smallest of these three values to be the stable radius, R_{stab}, of the core, knowing that if a test particle is within the smallest distance from the core, it also is within the two larger stability radii..
($1.50 \times 10^{12} < 3.05 \times 10^{12} < 6.14 \times 10^{12}$, $R_{stab} = 1.50 \times 10^{12}$ cm)

3.2.2 Calculating the Energy Restrictions

If the test particle does not fall within the stable radius of the core, then I automatically exclude it from the accretion area. Falling within the stable radius, however, does not guarantee that the particle will be captured. If the particle cannot dissipate its kinetic energy relative to the core during its encounter with the stable radius (or dissipates its energy too quickly and cannot enter the Bondi radius) then it will not be able to accrete, regardless of whether it falls within the stable radius of the core (see Chapter 2.7 for a deeper discussion of this subtlety).

The first step is to determine the relative sizes of the stable radius and the Bondi radius, which will tell whether the particle needs to dissipate all its energy or hold on to some energy.

Bondi Radius

First, I calculate the Bondi Radius of the core, using the equation:

$$R_{bondi} = \frac{Gm_{core}}{{c_s}^2} \tag{3.32}$$

($R_{bondi} = 2.48 \times 10^{11}$ cm)

The Bondi radius describes the possible radius of an atmosphere on that core, within which orbiting gas particles would have sub-escape energies.

Determining the Crossing Radius

If the core's stable radius is the larger of the two, then the test particle has distance $2R_{stab}$ in which to dissipate its energy. If the Bondi radius of the core is larger, however, the work done is not over

the stable radius – rather, the particle must not couple to the gas within the distance of $2R_{bondi}$. Thus, the crossing radius – or the radius used to determine the work done by gas drag – is the larger of the Bondi and stable radii, in all cases.

($1.50 \times 10^{12} \geq 2.48 \times 10^{11}$, $R_{cross} = 1.50 \times 10^{12}$ cm)

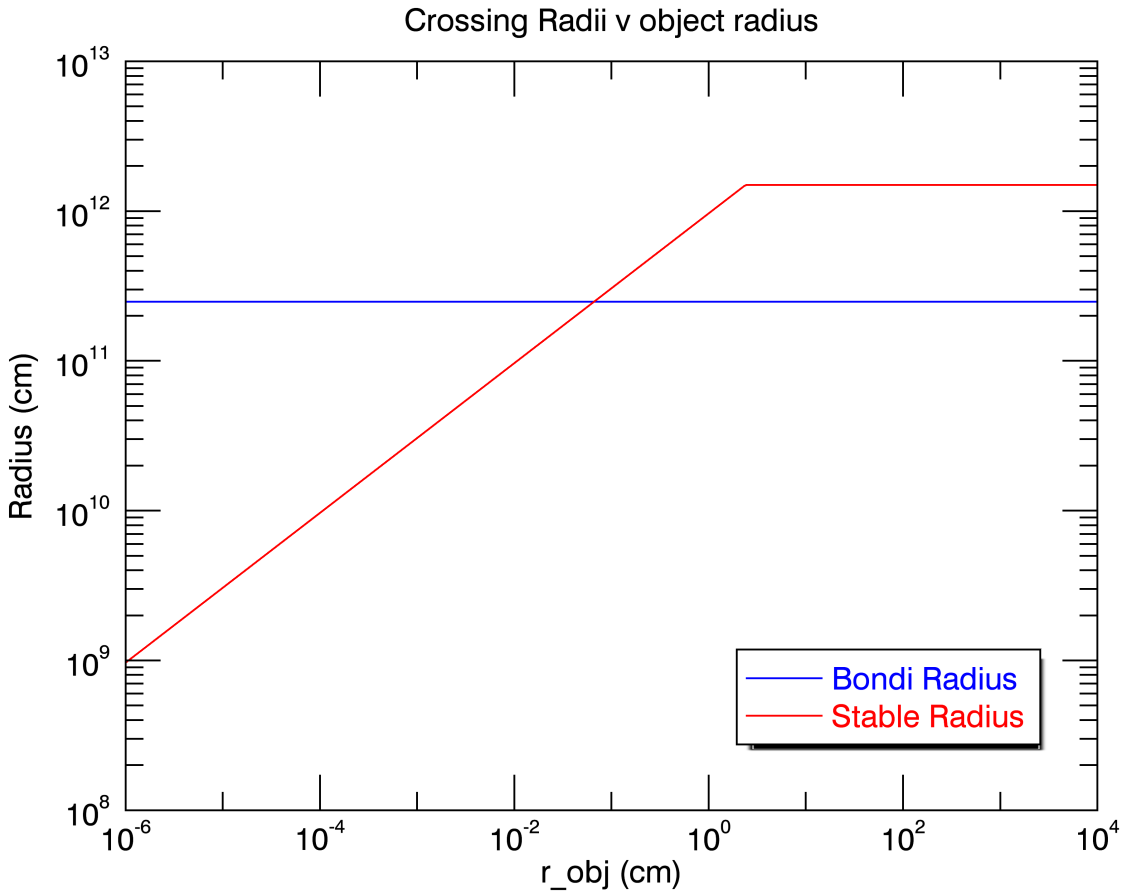

Figure 3.8: Comparison between Bondi radius and stable radius for a given test object. When the Bondi radius is larger than the stable radius, the length scale that determines the accretability is the Bondi radius. When the stable radius is larger, it is the determining length scale.

Velocity Adjustment

In order to determine the energy dissipation, I must first be able to specify what the energy of the object will be as it encounters the core. At an infinite distance from the core, this will simply be dependent on its terminal velocity. Yet as described in Chapter 2.8, as the object encounters the core, it will exchange potential and kinetic energies, and could possibly be accelerated to a higher

velocity.

The crossing radius will determine whether the object will be accelerated or not. I find the velocity associated with a particle located at R_{cross} from the core (using the reasoning in Section 2.8) and compare this velocity, v_{cross} with the object's v_{oc} at ∞. I then can specify that:

$$v_{enc,core} = \max\{v_{oc},\, v_{cross}\} \tag{3.33}$$

$$v_{enc,gas} = \max\{v_{og},\, v_{cross} + v_{core} - v_{gas}\} \tag{3.34}$$

Where $v_{enc,core}$ is the relative velocity between the core and the object upon encounter, and $v_{enc,gas}$ is the relative velocity between the object and the gas upon encounter with the core.

These encounter velocities will help to determine the energy constraints on the incoming particle.

Energy Dissipation due to Gas Drag

Next, I calculate the work done due to drag force. I use the equation:

$$W = -\Delta E = F\Delta d \tag{3.35}$$

In this case, the distance, d, is R_{cross}. In order to determine the force, F, I consider the force due to drag on the particle (determined by drag regime – see Chapter 2.6) at the particle's encounter velocity, $v_{enc,gas}$ (after the particle has been accelerated, if it is so). In reality, the velocity is some complicated function of the drag force and its potential energy – after all, drag force from gas acts on it **as** it is accelerated by the gravity of the core. The object might not get the chance to accelerate fully to its encounter velocity. If the object does not accrete, however, then it will definitely be at v_{enc} at the end of its encounter. Thus, allowing it to accelerate before being acted upon by gas works for the sake of excluding particles (though it might miscalculate the drag force on particles that would have accreted anyway). Thus, the change in energy is given by:

$$\Delta E = F_d R_{cross} \tag{3.36}$$

plugging in $v_{enc,gas}$ for v_{rel}. ($\Delta E = 2.16 \times 10^{13}$ ergs)

Now, I calculate the kinetic energy of the particle at infinity – essentially, from the perspective

of the core, what is the energy the particle has to lose to couple to the gas? The kinetic energy of the particle at infinity is given by:

$$KE = \frac{1}{2} m_{obj} v_{\infty}^2 \tag{3.37}$$

where v_{∞} is the object's velocity relative to the core before the encounter – v_{oc}. For small particles, which are moving at essentially the same velocity as the gas, this approaches v_{cg}. For large particles, which are moving at essentially the same velocity as the core, this will be 0.

($KE = 3.13 \times 10^9$ ergs)

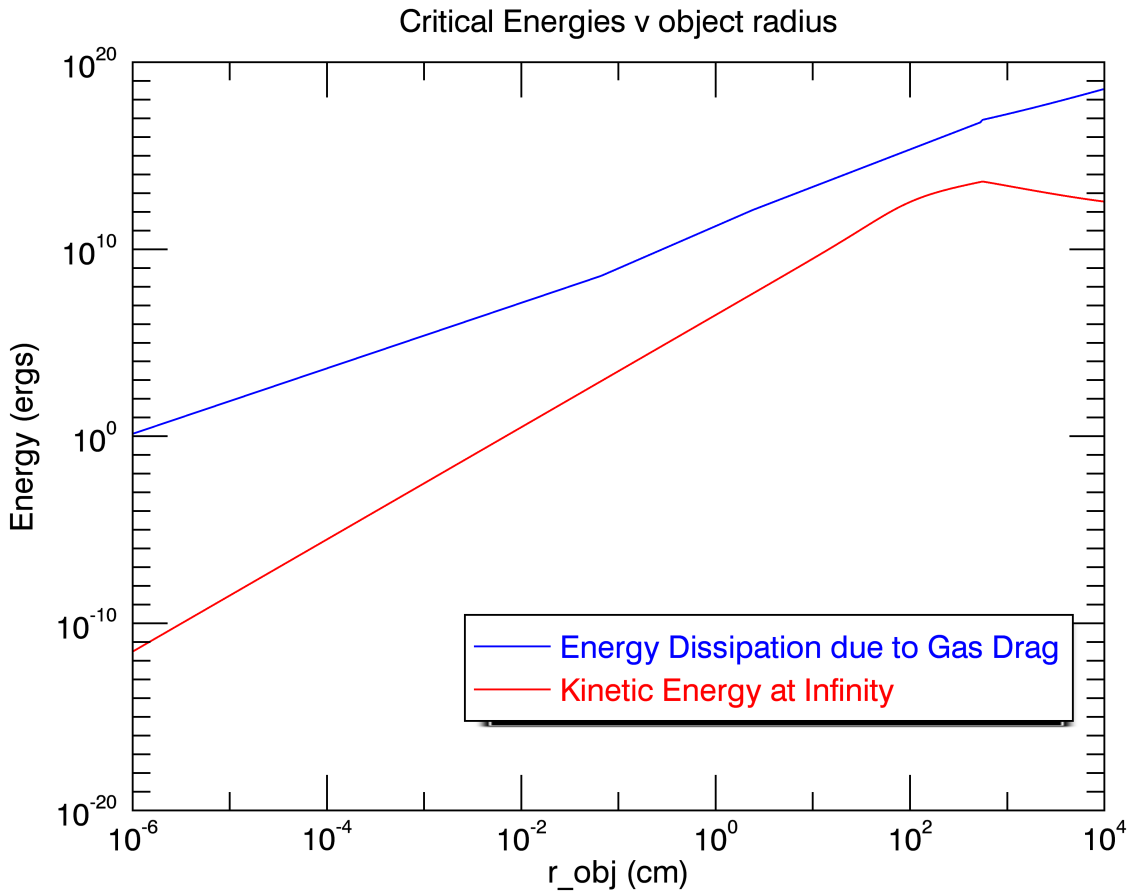

Figure 3.9: Graph depicting the kinetic energy of a test object at ∞ (relative to the core) and the energy dissipation due to work done by gas drag. Where the energy dissipation is greater than the kinetic energy at infinity, the test object will be gravitationally bound to the core by the end of the encounter.

3.2.3 Determining Accretablility

Once I have the stable radius, the size of the Bondi radius, the work done by drag over the crossing radius, and the kinetic energy of the particle at infinity, I can calculate whether that specific particle will accrete or not. First, I impose the condition that the particle is within R_{stab}. Next, I impose the energy conditions, explained in Chapter 2.7. Thus, the three conditions are:

$$|a_{obj} - a_{core}| \leq R_{stab} \tag{3.38}$$

$$\text{If } R_{stab} \geq R_{bondi},\ F_d(v_{enc,gas})R_{stab} \geq \frac{1}{2}m_{obj}v_{oc}^2 \tag{3.39}$$

$$\text{If } R_{stab} \leq R_{bondi},\ F_d(v_{enc,gas})R_{bondi} \leq \frac{1}{2}m_{obj}v_{oc}^2 \tag{3.40}$$

If that particle satisfies both the radius and the energy condition, then I add that particle to the area of accretion. Summing over all test particles of a certain size will give me a range of accretion.

3.2.4 Calculating Growth Timescale

Once I have the area of accretion, I can plug into the equation for growth timescale (Equation 3.9). The area of accretion is roughly rectangular. I use the limits of accretion to determine the length of the accretion rectangle.

To determine the height of the accretion rectangle (and to determine the scale height for accretable material), I take the minimum of the stable radius and H_d, the height of the dust at that particular point in the disk. Thus, if the stable radius is small enough to fit within the disk on all sides, then it can fill completely. If, however, the disk is very thin, or the stable radius very large, then the accretion will be cut off above and below the core. I assume the height of the disk using Kelvin-Helmholtz shear instability (Helmholtz, 1888) to arrive at the equation:

$$H_d = \left(\frac{H_{gas}}{a_{core}}\right)^2 a_{core} \tag{3.41}$$

($H_d = 2.71 \times 10^1 1$ cm)

($1.50 \times 10^{12} > 2.71 \times 10^{11}$)

Essentially, this represents the minimum height dust settling can produce without the shear between the dust layer and the gas only layer creating instability, causing the dust layer to expand (e.g.

Papaloizou & Pringle, 1985, Johansen et al. 2006).

I multiply Σ by the fraction of dust to gas $f_{accrete}$ (typically about 1%) to find the surface density of accretable material. I then divide by H_d, since all the accretable material will be within this height, to get a volumetric density of accretable material. Using the accretion area $A_{accrete}$ I thus have found the timescale of growth for the core.
(timescale $= 1.83 \times 10^4$ yrs)

Gravitational Focusing Timescale

As a comparison, I follow the steps outlined in Chapter 2.2 to find the corresponding timescale of growth using the gravitational focusing method. For v_{rand} (the encounter velocity of the incoming particle) I use v_{Hill}, using the assumption of previous (unsuccessful) encounters between the particle and the core. Plugging in πb^2 for $A_{accrete}$ and using Equation 3.10 yields the gravitational focusing timescale.
(timescale $= 2.51 \times 10^6$ yrs)

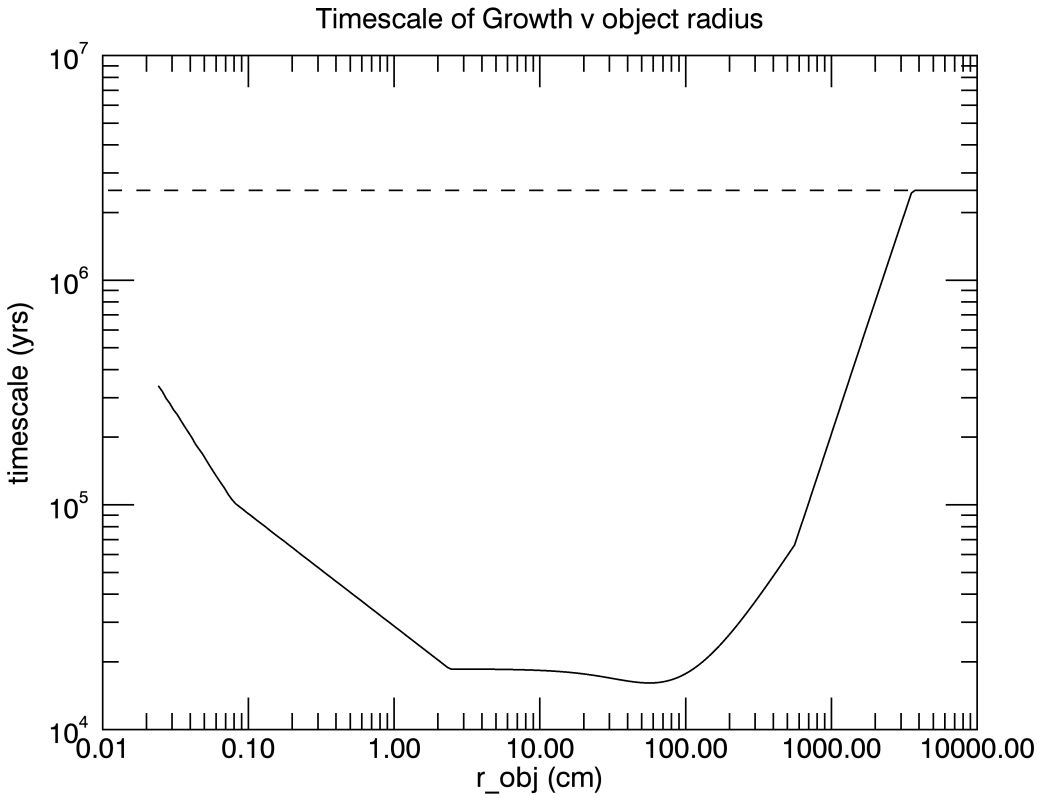

Figure 3.10: Timescale of growth v object radius. At the small end of the graph (where $r_{obj} < 0.01$ cm), no particles will satisfy the energy constraints, since they will all be coupled to the gas. Therefore, the timescale of growth grows to infinity, and planet growth in this regime of disk particles is impossible.

In this final graph, one can see all the elements of the model coming into play. At the left side, the line is cut off at about 0.02 cm. This is not a product of the graphing range, but rather a product of the physics itself. At this point, particles are so small that they couple completely to the surrounding gas. Since at this small size, the Bondi radius is larger than the stable radius, the fact that particles are coupled to the gas means they cannot enter the Bondi radius, so will never be able to get inside the stable radius. At these size scales, timescales of growth will be infinite.

When particles are able to accrete onto the core, in this example, all particles within the stable radius are able to accrete, so the timescale of growth is affected mainly by the stable radius and by v_{oc}. Smaller than 2 cm in radius, the WISH radius is smaller than the Hill radius and timescales are lengthened accordingly (the kink in the line at 0.1 cm corresponds to a shift between gas drag

regimes). Above 2 cm, accretion is set by the Hill radius. Here, particles are moving at roughly the gas velocity, but are large enough that through their gravitational interaction with the core, they can decouple and accrete. At around 80 cm, in fact the exact location of the "meter-sized barrier", particles have a maximum relative velocity with respect to the core due to their rapid radial motion, and as such, this corresponds to a minimum in timescales of growth.

After this, the particles are no longer moving with the gas, resulting in decreased v_{oc} and thus longer timescales. At the right side where the line levels off, the particles are so large that they are not particularly affected by the gas, so the gravitational focusing model (and growth timescale) is a better approximation than the gas-dominated model.

Chapter 4

Exploring Parameter Space

Now that I have developed the model, I explore parameter space to find out what kinds of variables are most important for efficient core growth, as well as figure out what kinds of constraints I can put on searching for gas giant formation in extrasolar systems.

I vary four parameters: the size of the star, the starting size of the core, the distance from the star to the core, and the density of the disk, in order to try to get a complete picture of the dynamics of the system. For this study I have shown the timescale of growth using a $5m_{earth}$ core. This is the size of the "last doubling" timescale, assuming the core starts rapid accretion of a gas envelope at about $10m_{earth}$. Thus, this is the last (and most time intensive) doubling the core needs to complete in order to begin accreting gas.

My default parameters are $M_{star} = M_{sun}$, $a_{core} = 10$AU, and the temperature and disk surface density profiles used in the previous chapter (Equation 3.1) to model the solar system.

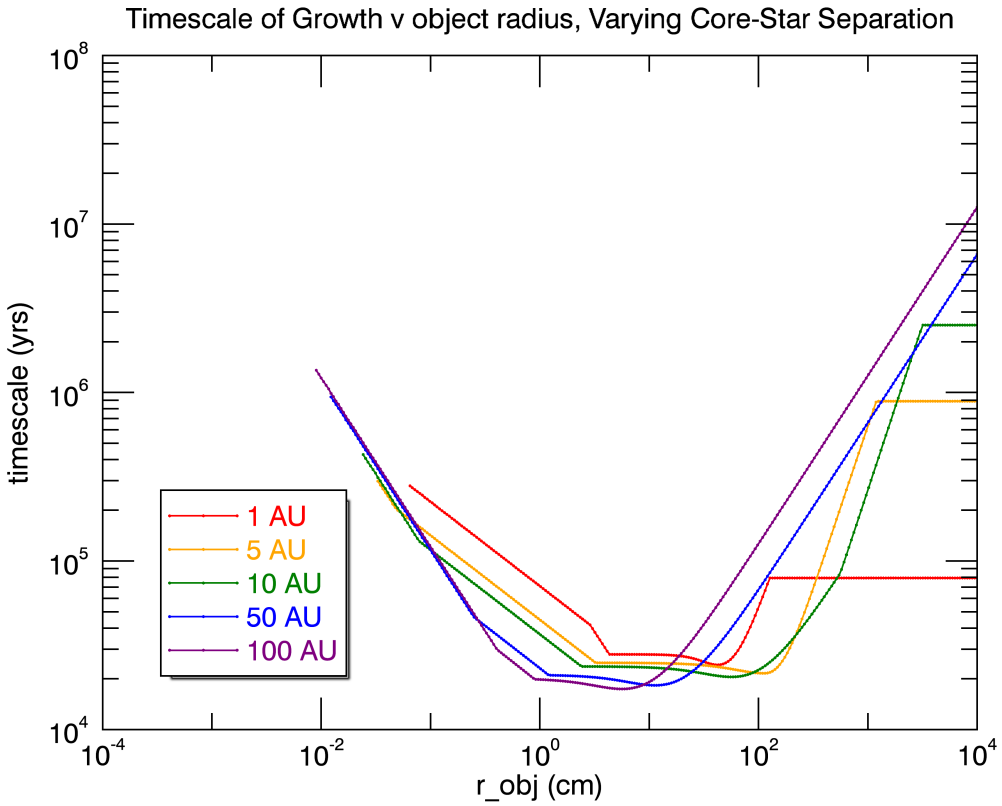

Figure 4.1: Timescales of growth, varying separation between core and central star. Assuming $m_{core} = m_{earth}$, gas density = solar system, $M_{star} = M_{sun}$.

Figure 4.1 shows the dependence of timescale of growth on separation between the growing core and the central star. The most surprising part of the model is in fact that larger separations from the central star, in general, have lower timescales of growth. Not only this, but at larger timescales, small particles are more likely to accrete onto the core. For example, at 1 AU, particles smaller than about 0.1 cm cannot accrete onto the core. At 100 AU, however, particles down to 0.01 cm – about ten times smaller – are able to accrete onto the core, with timescales below 1×10^6. This is because at larger separations, the density of gas is lower, making it easier for particles to decouple from the gas during their encounter with the core and subsequently enter the stable radius.

For a similar reason, however, closer-in cores have lower timescales for larger particles. This is because denser gas environments are able to slow down these particles more effectively, increasing v_{oc} and thus increasing the rate at which the core encounters particles in its orbital path.

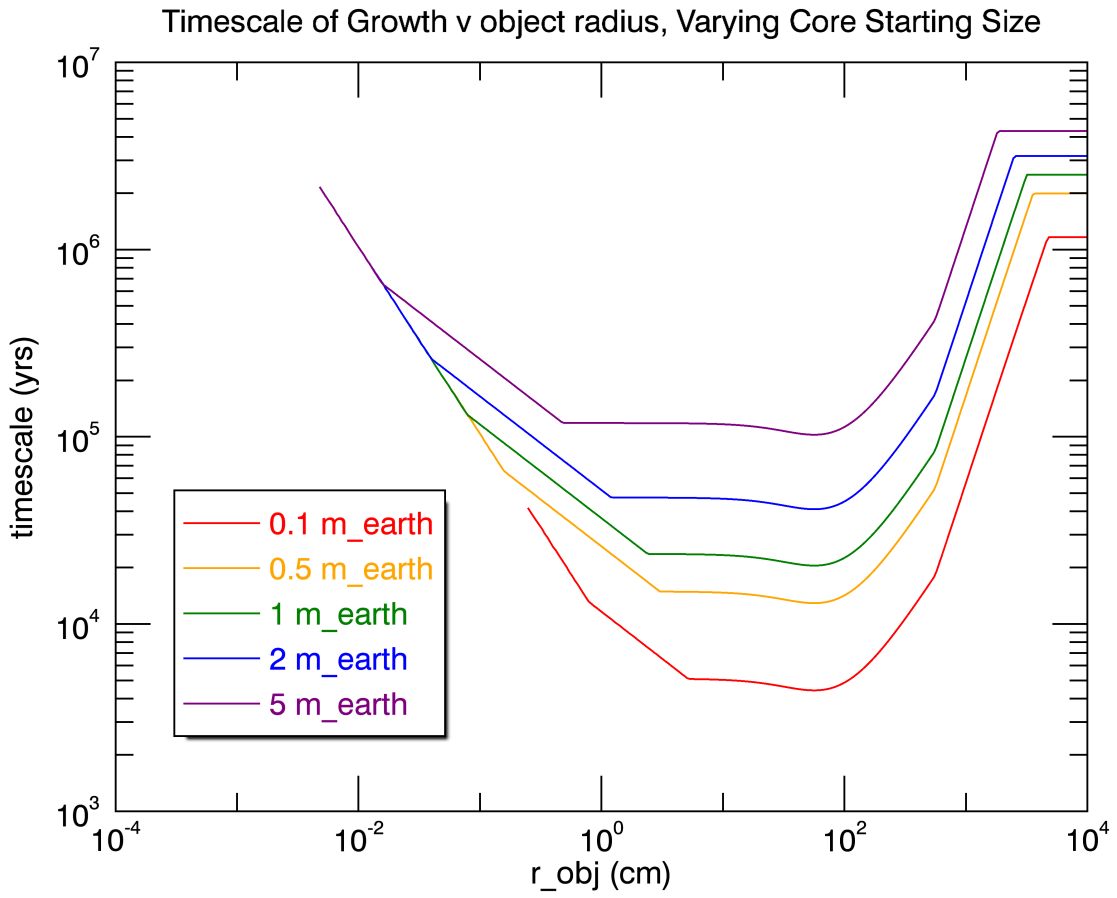

Figure 4.2: core mass varies. Assuming gas density = solar system, $M_{star} = M_{sun}$, $a_{core} = 10au$.

Timescales of growth also depend on the size of the growing core. Larger cores have larger timescales of growth. In addition, smaller cores shift the switch from WISH radius to Hill radius to the right. This makes intuitive sense. The gravity of smaller cores accelerates particles more weakly, so they are less able to overcome gas drag acceleration. Thus, the WISH radius is smaller for smaller cores (compared to the Hill radius), shifting the switch to the right.

The point of smallest timescale is not affected by core size. This also makes intuitive sense. The point of smallest timescale corresponds to the point at which the relative velocity between the core and the object is maximized. Since I assume the core to be moving at its Keplerian velocity, the low point is simply a factor of v_{og}, independent of core mass.

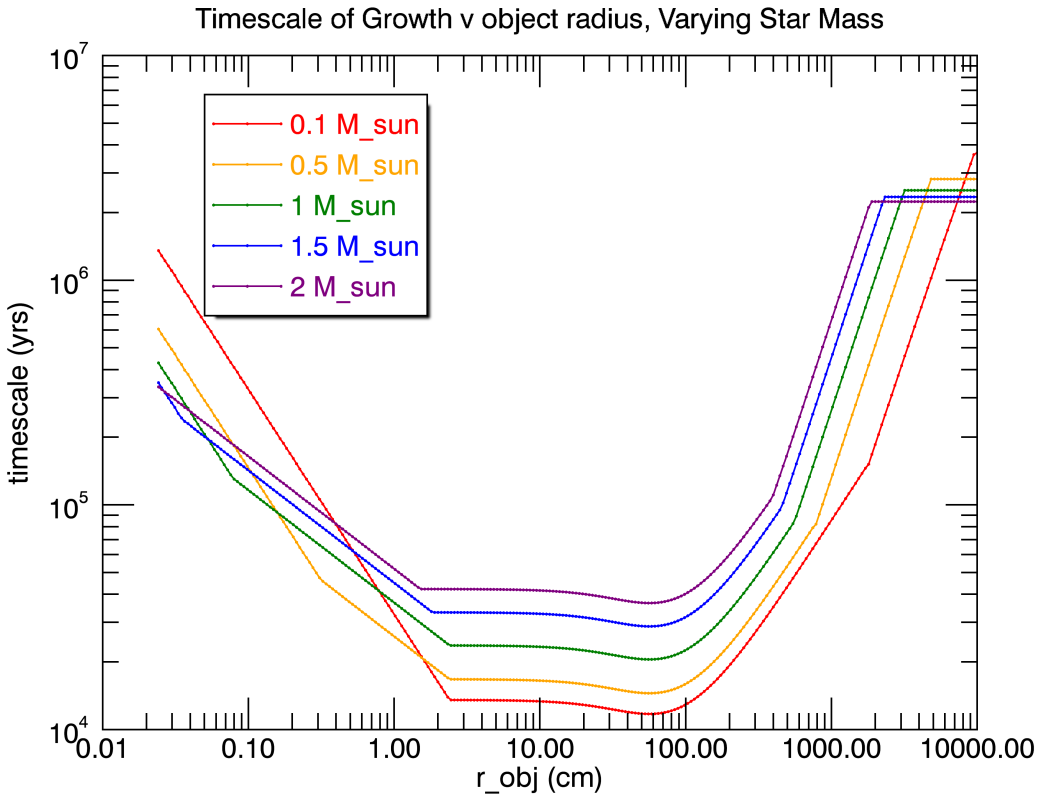

Figure 4.3: Timescales of growth, varying mass of star (dynamical changes only, temperature profile remaining same). Assuming $m_{core} = m_{earth}$, gas density = solar system, $a_{core} = 10au$.

Star mass certainly has an effect on the timescale of growth of cores. Larger stars generally produce longer timescales of growth than smaller ones (in the range of particle sizes that produces a mostly flat curve). This is counterintuitive, because larger-mass stars have shorter dynamic timescales – objects will orbit faster. But two important factors can explain this correlation. First, as star size increases, R_{Hill} decreases, all other things being equal. Thus, the core has a smaller area within which particles have even a chance of accreting. Furthermore, the correction to the orbital velocity of the gas goes inversely with the orbital velocity of the core (see Chapter 2.4). Thus, when the star size increases and the orbital velocity of the core increases, v_{cg} decreases, meaning the core will encounter gas-coupled particles less frequently. This explains why larger stars produce larger timescales of growth.

When particles are small, however, and accretion is based on the WISH radius, a more complicated relationship holds. It seems that up to a certain point, the timescales of growth will decrease

with increasing star size, and then after that point, will increase with increasing star size.

In order for this information to be useful, however, one would have to incorporate a relationship between star size and disk properties. It is naive to assume that star size would not impact the properties of the disk itself (temperature and surface density profiles).

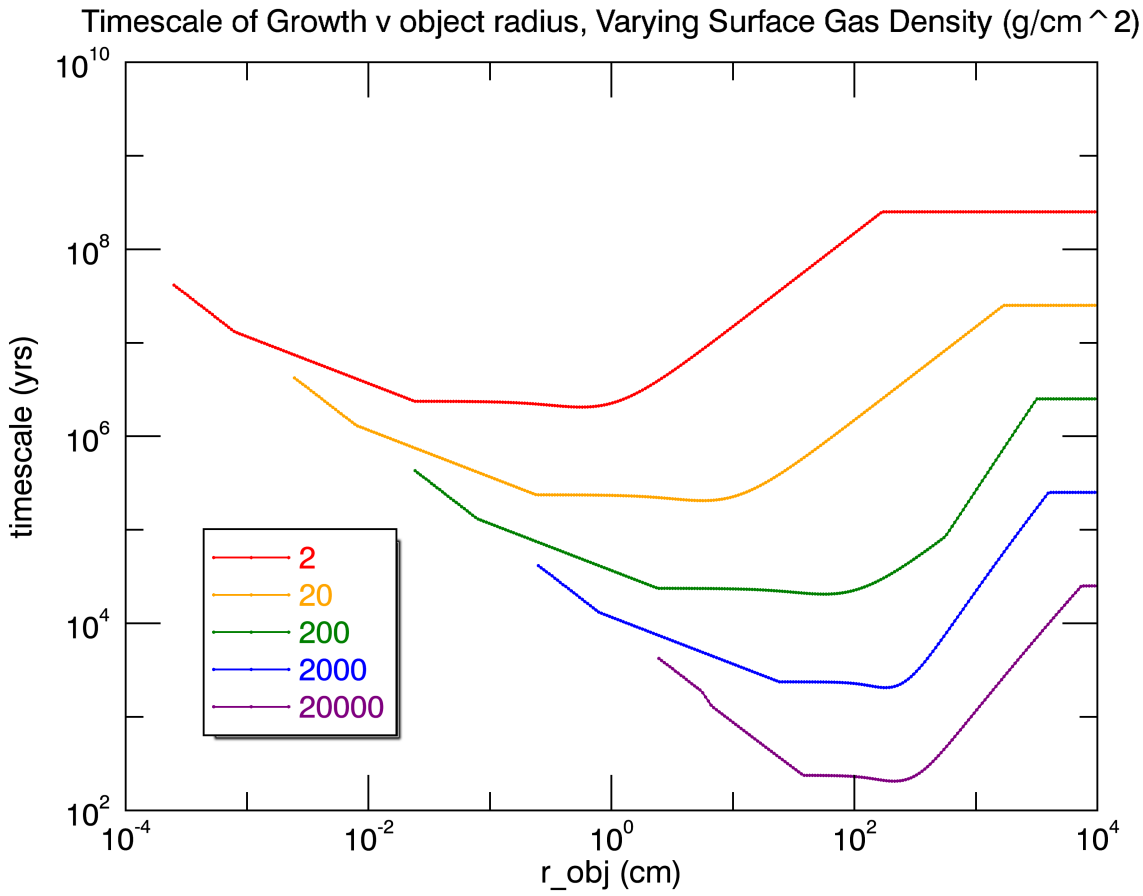

Figure 4.4: gas surface density varies. Assuming $m_{core} = m_{earth}$, $M_{star} = M_{sun}$, $a_{core} = 10au$.

Finally, when gas density changes, the timescale of growth changes accordingly. Generally, as gas density increases, timescale of growth shifts down. This is simple – with more gas comes more accretable material, and thus more rapid growth. As gas density increases, too, the switch from the WISH radius to the Hill radius shifts rightward – more gas means more gas drag, so smaller WISH radii (and thus WISH-dominated dynamics for larger particles). As that switch point moves rightward, small particles are less likely to be accreted. Finally, as gas density increases, the

timescale of growth minimum shifts to the right (larger particle sizes). Denser gas means more gas drag, and thus the particular size particle that satisfies the "meter barrier" problem increases.

What can be said in general, then, about core-accretion growth using the results of this study? For one, timescales of growth are reduced from those estimates given by the gravitational focusing model for a large range of particles. In particular, cores "prefer" to accrete small particles in a Hill radius dominated region – that is, particles that are coupled to the gas at ∞, enter the stable radius like that, and then spiral in to collide with the core. The most effective growers are those particles that have a large radial velocity component, increasing the relative velocity between them and the core.

Finally, the gas model developed in this paper breaks down for larger particles, where gas has little effect on their velocity. At these sizes, gravitational focusing is the correct way to describe their accretion onto the core. These models could prove useful for future predictions of early characteristics of systems with known large-separation gas giants, as well as a possible way of predicting whether a native gas-giant could exist in a given system, given the values of the various parameters.

Chapter 5

Case Study – HR8799

I now apply the model to the case of HR8799 planetary system, which will test the extreme limits of my hypothesis of gas giant core growth through accretion.

5.1 Motivation

As previously stated in the introduction, this system will test the limits of my model by presenting a case of planets with exotic properties, challenging the scientific community to either explain their formation through accretion or through gravitational instability (neither of which, in its present form, can fit the planets into the model nicely).

The system is composed of an A-type star, orbited by four planets, three of which (HR8799b, c, and d) are gas giants located at a distance of more than 20 au from the central star. The masses of the three gas giants, as stated in the discovery paper, are 7, 10, and 10 times the mass of Jupiter respectively, or 1.329×10^{31}, 1.898×19^{31}, and 1.898×10^{31} grams. The dilemma, of course, is that the planets are too big and far away to be described by conventional models of planetary accretion, and too small to be described by gravitational instability collapse models. The following graph (Kratter, Murray-Clay, and Youdin, 2010) describes the problem pictorially:

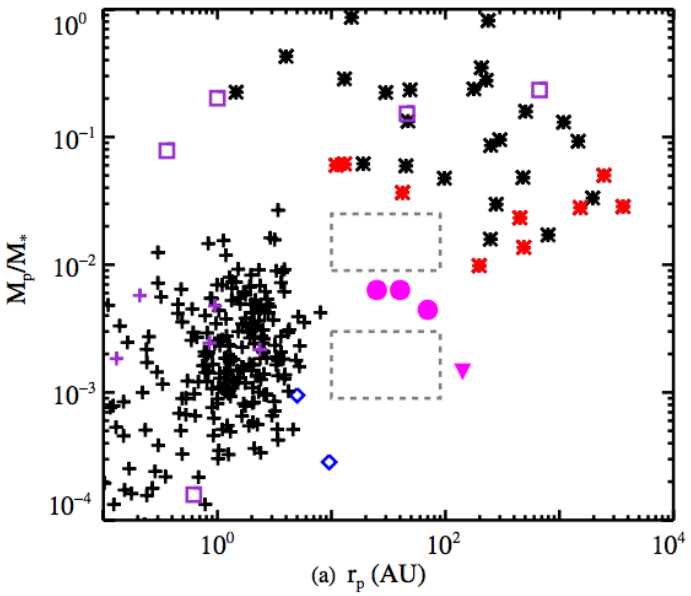

Figure 5.1: Taken from Kratter, Murray-Clay and Youdin, 2010, Figure 6. Plot of fractional mass of the object v distance from central star. Substellar companions are shown as asteriskses and planets, formed by accretion, are shown as plusses. HR8799 system shown as pink circles.

The HR8799 planets fall right between the two populations – planets formed by core accretion and stellar companions, formed by a variety of other processes. In applying my model to the system, I can figure out which population they should belong to.

5.1.1 Choosing Parameters

To begin, I must find out what the appropriate parameters are to plug in. I need to determine the following values in order for the model to have minimal uncertainty:

1. Mass of the star at the time of accretion
2. Distances of the planetary cores, assuming no drift
3. Size of accreting particles
4. Gas density in the disk
5. Temperature profile of the disk
6. Current age of the planets

From the discovery paper, I extract the distances and masses/radii of the planets (Marois et al., 2010). Furthermore, from a follow-up paper done by Marley et al. (2010) I find the ages of the planets, which will be, roughly, the limiting timeframe of accretion. Below is a table specifying each value for the planets:

	HR8799 b	HR8799 c	HR8799 d
a_{core}	68 AU	38 AU	24 AU
$Mass\,(M_{Jupiter})$	7	10	10
$R(R_{Jupiter})$	1.2	1.2	1.2
Age	360 Myr	40-100 Myr	30-100 Myr

Figure 5.2: Parameter values specific to HR8799 b, c, and d. Information taken from Marois et al. 2010 and Marley et al. 2010, through observation and theoretical modeling.

Furthermore, Kratter, Murray-Clay and Youdin (2010) modeled the temperature profile and density profile of the disk, as well as the projected mass of the star when accretion would have begun. They model the disk as passively irradiated following the work of Chiang and Goldreich (1997), thus introducing an $a^{-3/7}$ dependence for temperature. Furthermore, they follow a conservative accretion model for the star, working backwards under the assumption that the star follows a typical mass-luminosity function for an A-type star and accretes a constant 10^{-7} M_{sun} per year. This rate was set based on the minimum requirements for star formation timescales. The parameters relating to the stellar environment are summarized in the table below:

	HR 8799
Temperature profile	$40\text{K}\,(\frac{a_{core}}{70\text{AU}})^{-3/7}$
Disk density profile (minimum)	$200\,g/cm^2(\frac{a_{core}}{AU})^{-1}$
Disk density profile (maximum)	$\frac{c_s\,\Omega}{\pi G}$
M_{star} (minimum)	$1.35\ M_{sun}$

Figure 5.3: Parameter values specific to HR8799 system. Information taken from Kratter, Murray-Clay and Youdin (2010), through theoretical modeling.

$$\Sigma = 200\Big(\frac{a_{core}}{70\text{AU}}\Big)^{-1} \ \frac{\text{g}}{\text{cm}^2} \tag{5.1}$$

$$\Sigma = \frac{c_s \Omega}{\pi G} \ \frac{\text{g}}{\text{cm}^2} \tag{5.2}$$

For the gas density profile, I calculate the timescale of growth twice – once using the minimum gas density and once using the maximum – to get a sense of how dependent my hypothesis of core accretion is on accurate determinations of the early disks of planetary systems. My minimum gas density profile is based on the idea that the minimum amount of material present in a young disk is the amount of material in the current-day planets and asteroid belts of the system (Weidenschilling, 1977, Hayashi, 1981, and Desch, 2007). This is then adjusted to reflect the temperature of the A-type star. The maximum gas density profile is based on limits of stability of disks. At higher densities than those given by the Toomre condition, either rotational shear will stabilize the disk by expanding and thus restoring lower densities or it will collapse as in gravitational instability models (Kratter, Murray-Clay & Youdin 2010). Thus the maximum density is when the Toomre condition is exactly 1.

In terms of particle size, I assume that the disk is made of uniformly-sized particles. Possible future work will be to use a distribution of particle sizes. I also assume that the cores uniformly begin at $m_{core} = 5m_{earth}$ (as seen in the previous chapter, as core mass increases, so does timescale of growth. Thus, by using the "last doubling" timescale, I can judge the success of the model in a conservative way). Finally, I use the values below as reference to convert the masses to grams (instead of with respect to the sun and Jupiter):

$$M_{Sun} = 1.9891 \times 10^{33} g$$

$$M_{Jupiter} = 1.898 \times 10^{30} g$$

$$1AU = 1.496 \times 10^{13} cm$$

5.2 Results

I represent the results of the simulation in a table form below:

	Σ (local disk surface density) (g/cm^2)	T (local disk temperature) (K)
HR 8799b	Min: 29.41 Max: 64.55	40.5
HR 8799c	Min: 52.63 Max: 175.03	51.97
HR 8799d	Min: 83.33 Max: 384.80	63.28

	(accretion radius of 5M_earth core) (gravitational focusing)(cm) $R_{accrete}$	(accretion radius of 5M_earth core) (gas disk model)(cm) $R_{accrete}$
HR 8799b	1.95x10^11	Min: 1.74x10^13 Max: 1.74x10^13
HR 8799c	1.46x10^11	Min: 9.72x10^12 Max: 9.72x10^12
HR 8799d	1.16x10^11	Min: 6.14x10^12 Max: 6.14x10^12

	τ (timescale of growth, gravitational focusing model) (yrs)	τ (timescale of growth, gas interaction model) (yrs)
HR 8799b	Min: 7.61x10^7 Max: 3.47x10^7	Min: 4.88x10^4 Max: 2.31x10^4
HR 8799c	Min: 3.18x10^7 Max: 9.56x10^6	Min: 4.64x10^4 Max: 1.54x10^4
HR 8799d	Min: 1.60x10^7 Max: 3.46x10^6	Min: 5.05x10^4 Max: 1.16x10^4

Figure 5.4: Results of core accretion simulations for HR8799 system. Assuming all accretable particles 10cm in radius. Min refers to the use of the minimum-mass disk density profile and Max refers to the use of the maximum-mass disk density profile. Realistic values will likely fall between these two models.

The gas-interaction model developed in this paper is largely successful. The timescales of growth

represent a significant reduction from the predictions using a gravitational focusing model. In all cases, the gas-interaction model predicts a timescale of growth well within estimations of lifetimes of disks. Reassuringly, all timescales of growth, including those modeled using the minimum mass solar nebula disk density estimate (the "upper limit" on the timescale of growth) are much less than the derived ages of the planets, which is more than can be said for the gravitational focusing timescales.

These timescales were generated assuming that all dust particles were of equal size. In reality, of course, there will be a variety of sizes of particles moving in the disk surrounding the core, following some sort of distribution. The timescales of growth of the HR8799 planets for varying particle sizes are shown in greater detail in the following graphs:

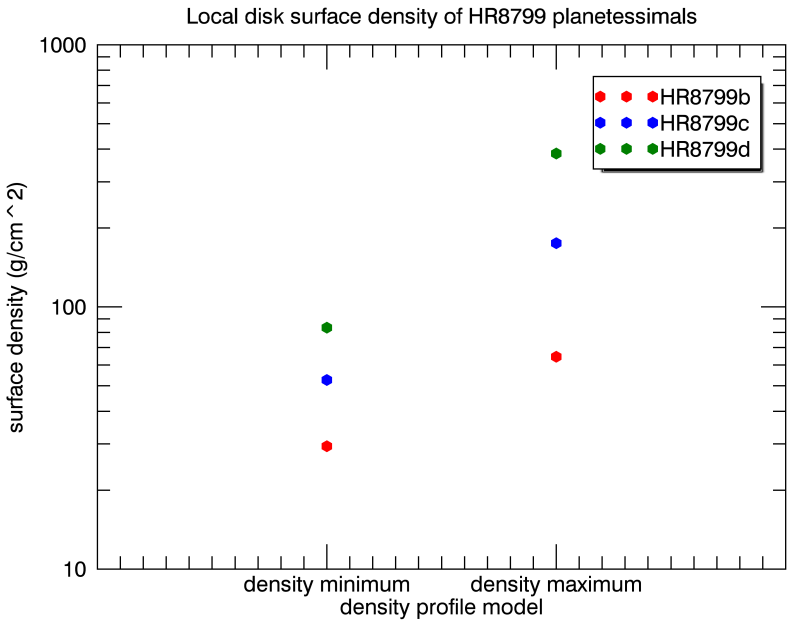

Figure 5.5: Local disk average surface densities (assuming laminar disk) around each core at the time of growth. Disk density is independent of particle size by assumption.

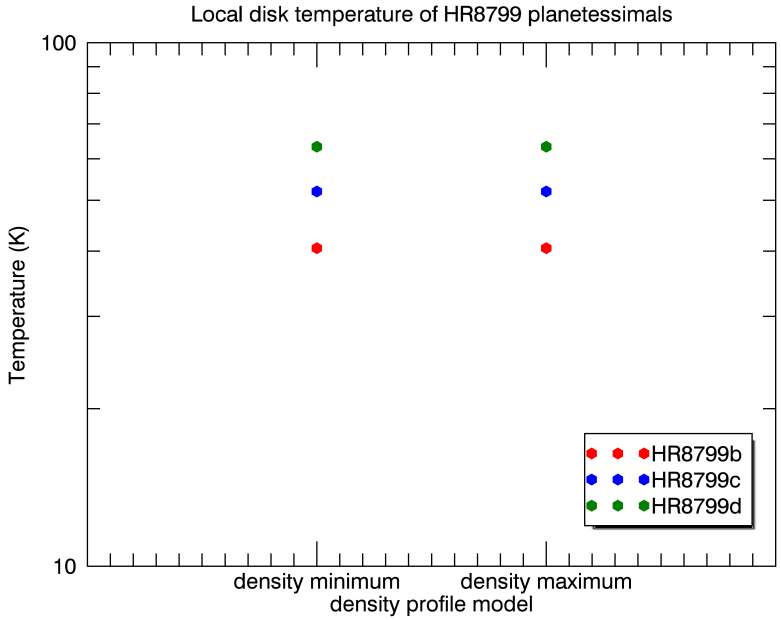

Figure 5.6: Local disk temperatures around each core at the time of growth. Disk temperature is independent of particle size (for the purposes of this model).

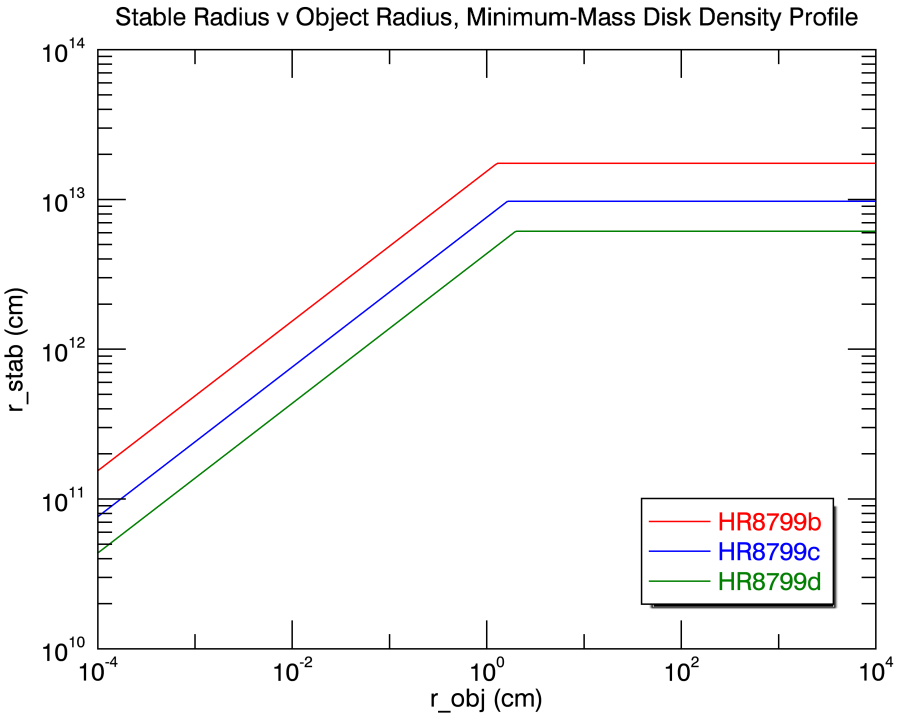

(a) Minimum disk density model.

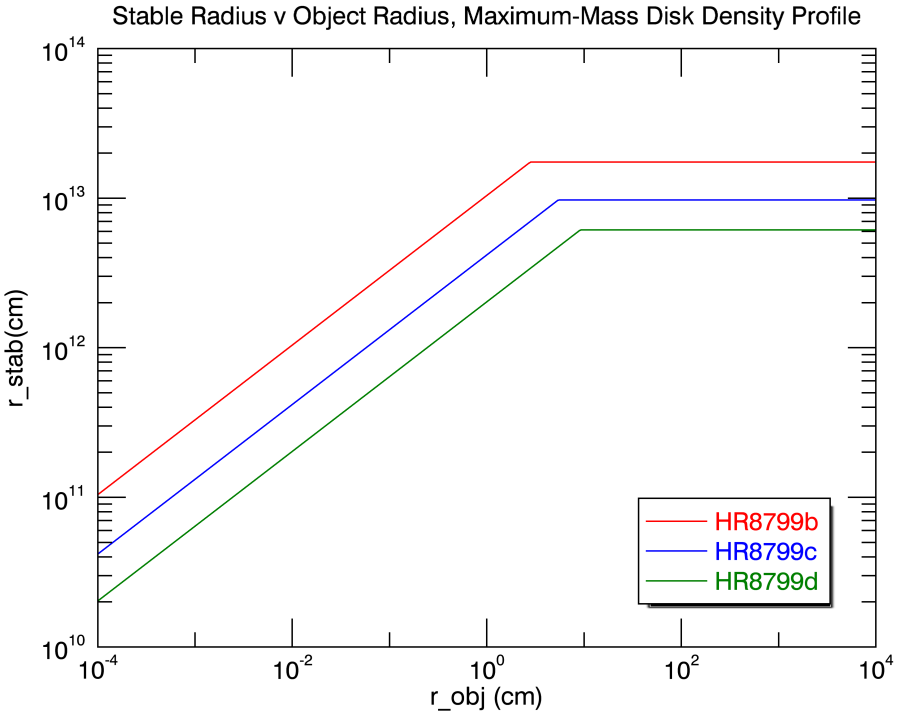

(b) Maximum disk density model.

Figure 5.7: Stable radii for the $5m_{earth}$ cores at the location of the HR8799 planets for different sized disk particles.

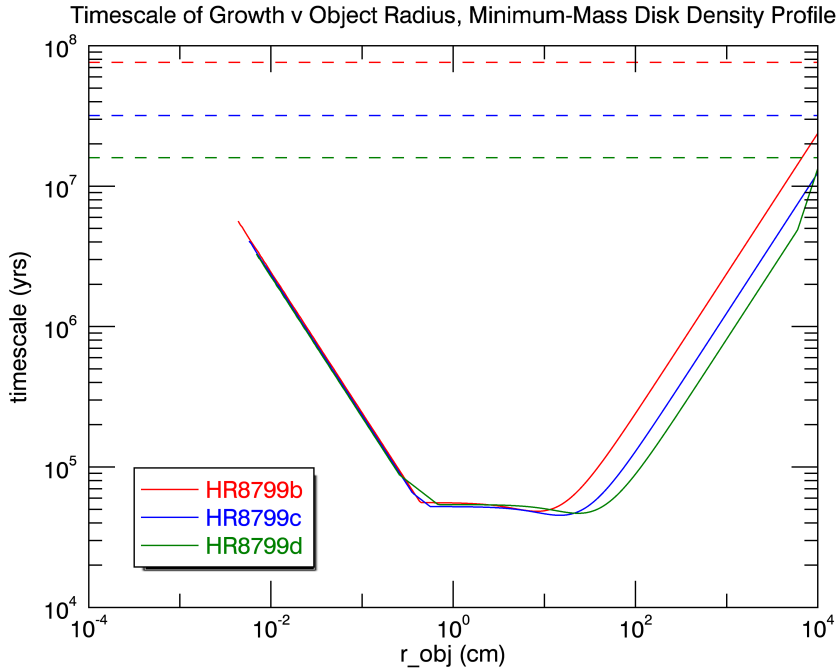

(a) Minimum disk density model.

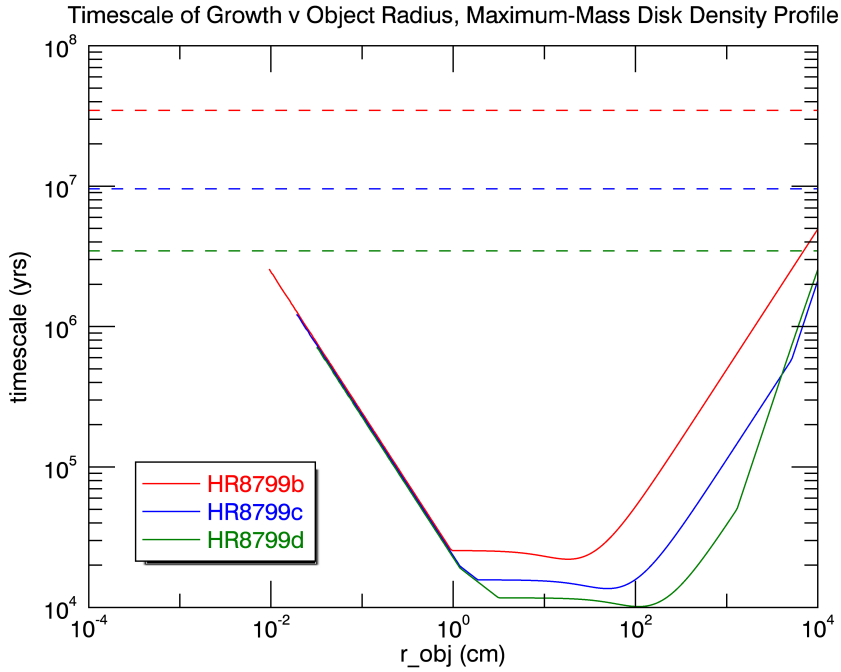

(b) Maximum disk density model.

Figure 5.8: Timescales of growth for $5m_{earth}$ cores at the location of the HR8799 planets, using the model developed in this paper. These timescales represent the "last doubling" timescale, or the last doubling needed before the core can enter the regime of rapid gas envelope accretion. Dashed lines show the timescale of growth following the gravitational focusing model.

As shown in the above figure, even if I assume worst case scenario (minimum density disk profiles), the particles in the disk would have to be uniformly less than 10^{-2} cm or larger than 10^{3} in radius in order for a core-accretion model to predict timescales larger than 10^{6} years for any HR8799 planet. Interestingly, all three planet cores have very similar timescales of growth in the minimum-density case. This reinforces the hypothesis that all three were formed the same way – either all three by core accretion, or all three by GI. The results of this research point to core accretion as the growth mechanism for the three gas giants, while the results of other studies (Kratter, Murray-Clay and Youdin, 2010) discourage GI as the mechanism.

Thus, I conclude my case study of HR8799 with a positive result – the model predicts that the large-separation gas giants are most likely formed as a result of core accretion.

Chapter 6

Conclusion

The study I present in this paper is quite successful. The goal was to use gas interactions to model the growth of gas giant cores at timescales shorter than the age of the protoplanetary disk. Specifically, I used the model to predict the timescales of growth of the HR8799 planets.

Using both a minimum disk density profile (based on the minimum mass solar nebula model) and a maximum disk density profile (based on the Toomre criteria) I was able to estimate the timescale of the last doubling of HR8799b,c, and d. These timescales were reduced from around 10^7 years (using gravitational focusing) to 10^4 years. Thus, timescales were within an acceptable range (less than 10^6 yrs) for particle sizes .01 cm to 10^3 cm. Of course, ultimate timescales of growth will depend on the particle size distribution within the disk, but as long as the majority of particles are within these limits, I can say that core accretion is a possible model for the growth of these planets.

Furthermore, delving into parameter space simulations of the model gave a good descriptive sense of what kinds of characteristics are conducive to large separation core growth. At small particle radii, the particles are not able to decouple from the gas during an encounter with a core to enter the Bondi radius. Thus, at the low end of particle sizes, the gaseous disk model predicts that timescales are infinite – these particles simply do not accrete at all. In general, the size of particle at which $R_{ws} = R_{Hill}$ up to the size at which the particles do not couple with the gas is the range at which core growth is most effective. The best growers were the size particles that presented the "meter barrier" problem – the size at which inward radial velocity is maximized (due to gas drag).

Thus, gas plays a vital role in influencing the path of colliding particles in the early and middle stages of giant planet growth. It limits the radius of stability of a core, by introducing an extra element of shearing force to approaching particles. It also increases the efficiency of accretion within that reduced radius of stability, by exerting forces on the particles that slow them down to relaxed velocities.

There is great potential for future work with this model, both in terms of adding more complexity and nuance and using it to help with observational efforts. Most importantly, a study that takes into account the various geometries present in the disk involving gas, the accreting particles, and the cores is needed. This, along with not being able to predict disk density profiles and particle size distributions, is the largest source of uncertainty in my modeling. In addition, protoplanetary disks are not perfectly laminar, and include both flares and turbulence, both which will have effects on the behavior of particles embedded in them. A direct extension of this project would be to incorporate models of turbulence in disks to further refine timescale estimates.

In terms of observation, this work could be used as a tool for predicting the separations of extra-solar gas giants from their stars (though this would ignore the fact that many planets drift considerable distances since their initial formation). Furthermore, it could be used to place constraints on properties of disks once a certain amount of core accretion takes place. For instance, if one size particle accretes well to the core and one does not, then you would expect to find increasing proportions of the latter surrounding a growing core.

My research does not provide a definitive proof of growth by core accretion. Just because the timescales of growth are correct does not mean my model describes the physical reality of how planetary cores grow. Our body of observational data on protoplanetary disk makeups, exoplanet systems, and their relationship is not nearly large enough for any theory on planet growth to be proven correct. Yet I believe that in showing possibility – even plausibility – I have paved the way for future work in the field.

Acknowledgements

There are many people who helped me to finish what has been the largest single project of my life. First and foremost, I want to thank my advisor, Ruth Murray-Clay, profusely. From countless

hours helping me to derive fluid dynamics equations on the board, to checking code again and again, each time finding one bug or another, she truly has been an amazing mentor and a guiding force in the project.

I'd also like to thank Professor Jim Moran, for keeping me on track and keeping my head in the right place during our weekly seminar meetings. Jim helped me to keep to my timeline and also make sure that I understood what I was doing well enough to explain it to others. Thank you to the Astro 99 students: Diana, Adrian, Caleb, and Brian – for struggling through it with me. Thank you to my external readers for your invaluable comments and suggestions.

Lastly, thank you to my friends and family, for bearing with me through the whole process. Thanks to my blockmates, who created "thesis thrones" in the Eliot House library and sat in them with me for the entire month of February. Thank you to my parents who care enough to struggle through 90 pages of theoretical physics and pretend they find it interesting. Special thanks to Richard Baxley who came up with the idea for the title. And thank you to the Center for Astrophysics and to the Harvard astronomy community in general.

Bibliography

[1] Adams et al., 1989, ApJ, 347: 959-975

[2] Alexander, R.D., Clarke, C.J. & Pringle, J.E. 2006, Mon. Not. R. Astron Soc. 369, 229-239

[3] Barman, T.S., Macinthosh, B., Konopacky, Q.M., & Marois, C. 2011a, ApJ, 733, 65

[4] Batchelor, G.K. *An Introduction to Fluid Dynamics*. Cambridge University Press, Cambridge, UK. 1967

[5] Batalha, N.M. et al., 2011, ApJ, 729, 27

[6] Batalha, N.M. et al., 2013, ApJ Supp. Series., 204:24

[7] Benz, W., 2000, Space Science Reviews, 92: 279-294

[8] Blum, J. & Wurm, G., 2000, Icarus, 143, 1

[9] Borucki, W.J. et al., 2010, Science, 327, 977

[10] Boss, A.P. 2011, ApJ, 731, 74

[11] Brown, P.P., & Lawler, D.F. 2003, J. Environ. Eng., 129, 222

[12] Cheng, N.S. 2009, Powder Technol., 189, 395

[13] Chiang, E.I., & Goldreich, P. 1997, ApJ, 490, 368

[14] Chiang, E., & Youdin, A.N., 2010, Annu Rev. Earth Planet Sci., 38:493-522

[15] Currie, T. et al., 2011, ApJ, 729, 128

[16] Desch, S.J., 2007, ApJ, 671, 878-893

[17] Dodson-Robinson, S.E., Veras, D., Ford, E.B., & Beichman, C.A. 2009, ApJ, 707:79-88

[18] Dominik, C., & Tielens, A.G.G.M., 1997, ApJ, 480:647-673

[19] Fabrycky, D.C. & Murray-Clay, R.A., 2010, ApJ, 710:1408-1421

[20] Fischer, D.A., & Valenti, J. 2005, ApJ, 622:1102-1117

[21] Fressin, F., et al., 2012, Nature, 482, 195

[22] Galicher, R., et al., 2011, ApJ, 739, L41

[23] Gammie, C.F. 2001, ApJ, 553, 174-183

[24] Goldreich, P., Lithwick, Y., & Sari, R. 2004, Annu. Rev. Astron. Astrophys, 42:549-601

[25] Greenberg, R., Wacker, J.F., Hartmann, W.K., & Chapman, C.R. 1978, Icarus, 35, 1-26

[26] Hayashi, C., 1981, Progress of Theoretical Physics Supplement, 70, 35

[27] Hayashi, C., Nakazawa, K., & Adachi, I. 1977, Publ. Astron. Soc. Japan, 29, 163-196

[28] Helmholtz, H. von, 1888, Sitzungsberichte Akad. Wissenschaften Berlin, 3, 647-663.

[29] Ido, S. & Makino, J., 1993, Icarus, 106, 210-227

[30] Ikoma, M., Nakazawa, K., & Emori, H. 2000, ApJ, 537, 1013-1025

[31] Jayawardhana, R., et al., 2006, ApJ, 648: 1206-1218

[32] Johansen, A., Henning, T., & Klahr, H. 2006, ApJ, 643:1219-1232

[33] Kalas, P. et al., 2008, Science, 322, 5906

[34] Kratter, K.M., Murray-Clay, R.A., & Youdin, A.N. 2010, ApJ, 710, 1375-1386

[35] Kuiper, G.P., 1951, Proc. Nat. Acad. Sci. USA, 37, 1

[36] Lambrechts, M. & Johansen, A. 2012, A&A, 544, A32

[37] Laughlin, G. & Rozyczka, M., 1996, ApJ, 456: 279-291

[38] Levison, H.F. & Stewart, G.R., 2001, Icarus, 153, 1

[39] Lissauer, J.J., et al., 2011, Nature, 470, 53

[40] Madhusudhan, N., Burrows, A., & Currie, T., 2011, ApJ, 737, 34

[41] Marois, C., et al. 2008, Science, 322 1348-1352

[42] Marois, C. et al., 2010, Nature, 468, 1080

[43] Oppenheimer, B.R., et al., 2008, ApJ, 679: 1574-1581

[44] Ormel, C.W. 2013, Mon. Not. of the Royal Ast. Soc., 428, 4, 3526-3542

[45] Ormel, C.W. & Klahr, H.H. 2010, A&A, 520, A43

[46] Ormel, C.W., Spaans, M., & Tielens, A.G.G.M 2007, A&A, 461, 215-232

[47] Papaloizou, J.C.B. & Pringle, J.E., 1985, Mon. Not. R. astr. Soc., 213, 799-820

[48] Perets, H.G., & Murray-Clay, R.A. 2011, ApJ, 733, 56

[49] Rafikov, R.R., 2004, Astron. J., 128, 1348-1363

[50] Rafikov, R.R., 2005, Astrophys. J. 621, 69

[51] Rafikov, R. R. 2009, ApJ 704:281-291

[52] Safronov, V.S. 1969. *Evolution of the Protopanetary Cloud and Formation of the Earth and Planets.* Nauka, Moscow. English translation: NASA TTF-677. 1972

[53] Stevenson, D.J. 1982, Planet. Space Sci., 30, 8

[54] Sudol, J.J. & Haghighipour, N., 2012, ApJ, 755:38

[55] Toomre, A., 1964, ApJ, 139, 1217-1238

[56] Vigan, A. et al. 2012, A&A, 544, A9

[57] Weidenschilling, S.J., 1977, Mon. Not. R. Astron Soc., 180, 57-70

[58] Weidenschilling, S.J., 1980, Icarus, 44, 1

[59] Weidenschilling, S.J. & Cuzzi, J.N. 1993, in Protostars and Planets III, ed. E.H. Levy & J.I. Lunine, 1031

[60] Wetherill, G.W. & Stewart, G.R., 1989, Icarus, 77, 330-357

[61] Zuckerman, B., Forveille, T., & Kastner, J.H. 1995, Nature, 373, 494-496